# NONDESTRUCTIVE TEST TECHNIQUE DEVELOPMENT FOR THE EVALUATION OF BONDED MATERIALS

John R. Zurbrick, et al

Avco Systems Division

Prepared for:

Advanced Research Projects Agency
Naval Air Engineering Center

5 November 1971

# NONDESTRUCTIVE TEST TECHNIQUE DEVELOPMENT FOR THE EVALUATION OF BONDED MATERIALS

J.R. Zurbrick
E.A. Proudfoot
C.H. Hastings

For the Period

1970 October 5 to 1971 November 5

ADVANCED RESEARCH PROJECTS AGENCY
PROGRAM
ON
NONDESTRUCTIVE TESTING

AVSD-0494-71-CR

Contract No. N00156-71-C-0550
Naval Air Engineering Center
Philadelphia, Pennsylvania 19112

Prepared by

AVCO GOVERNMENT PRODUCTS GROUP
SYSTEMS DIVISION
201 LOWELL STREET
WILMINGTON, MASSACHUSETTS 01887

UNCLASSIFIED

Security Classification

**DOCUMENT CONTROL DATA - R & D**

(Security classification of title, body of abstract and indexing annotation must be entered when the overall report is classified)

| | |
|---|---|
| 1 ORIGINATING ACTIVITY (Corporate author)<br>Avco Government Products Group<br>Systems Division<br>201 Lowell St., Wilmington, Mass. 01887 | 2a. REPORT SECURITY CLASSIFICATION<br>Unclassified<br>2b. GROUP |

3 REPORT TITLE

Nondestructive Test Technique Development for the Evaluation of Bonded Materials

4 DESCRIPTIVE NOTES (Type of report and inclusive dates)
Contract Annual Report (1970 October 5 to 1971 November 5)

5 AUTHOR(S) (First name, middle initial, last name)
John R. Zurbrick
Edward A. Proudfoot
Carlton H. Hastings

| 6 REPORT DATE | 7a. TOTAL NO OF PAGES | 7b. NO OF REFS |
|---|---|---|
| 1971 November 5 | 59 | 10 |

| 8a CONTRACT OR GRANT NO | 9a. ORIGINATOR'S REPORT NUMBER(S) |
|---|---|
| N00156-71-C-0550<br>b PROJECT NO<br>c.<br>d | AVSD-0494-71-CR<br>9b. OTHER REPORT NO(S) (Any other numbers that may be assigned this report) |

10 DISTRIBUTION STATEMENT

| 11 SUPPLEMENTARY NOTES | 12. SPONSORING MILITARY ACTIVITY |
|---|---|
| | Advanced Research Projects Agency<br>Naval Air Engineering Center<br>Materials Dept.<br>Warminster, Pennsylvania 18974 |

13 ABSTRACT

The third annual period of research and development at Avco Systems Division into Nondestructive Tests for the Evaluation of Bonded Materials, sponsored by the Advanced Research Projects Agency, has continued the course set by the first and second year's studies, namely development of NDT techniques for characterizing metallic substrate surfaces.

Continued studies of the relative influence of parametric variables on bond strength has shown the overriding influence of surface free energy ($\gamma_s$) as compared with contact angle on prepared substrates. The effective strain value ($k_o$) was found to be very complex. Its empirical treatment as if it consists only of uniformly distributed axial strain is a possibly useful solution which permits linking bond strength primarily to surface free energies.

Also, during this third year, effort was devoted to development of nondestructive, optical, and spectrophotometric techniques for characterizing contaminants which frequently occur on substrate surfaces. Although the most sensitive techniques available were employed, they did not reveal correlations with bond strength variability observed.

DD FORM 1473

UNCLASSIFIED

Security Classification

Ia

UNCLASSIFIED

Security Classification

| 14 KEY WORDS | LINK A | | LINK B | | LINK C | |
|---|---|---|---|---|---|---|
| | ROLE | WT | ROLE | WT | ROLE | WT |
| Nondestructive testing | | | | | | |
| Adhesively bonded joints | | | | | | |
| Bond adhesive strength | | | | | | |
| Bond strength prediction | | | | | | |
| NDT technique development | | | | | | |
| White light specular reflection | | | | | | |
| Substrate surface free energy | | | | | | |
| Contact angle | | | | | | |
| IR spectrophotometry | | | | | | |
| UV spectrophotometry | | | | | | |
| Laser specular reflection | | | | | | |

UNCLASSIFIED

Security Classification

Ib

# NONDESTRUCTIVE TEST TECHNIQUE DEVELOPMENT FOR THE EVALUATION OF BONDED MATERIALS

J.R. Curbrick
E.A. Proudfoot
C.H. Hastings

For the Period

1970 October 5 to 1971 November 5

ADVANCED RESEARCH PROJECTS AGENCY
PROGRAM
ON
NONDESTRUCTIVE TESTING

**AVSD-0494-71-CR**

Contract No. N00156-71-C-0550
Naval Air Engineering Center
Philadelphia, Pennsylvania 19112

Prepared by

AVCO GOVERNMENT PRODUCTS GROUP
SYSTEMS DIVISION
201 LOWELL STREET
WILMINGTON, MASSACHUSETTS 01887

IC

## FOREWORD

This report was prepared by Avco Corporation, Systems Division, Lowell, Massachusetts, under sponsorship of the Advanced Research Projects Agency (ARPA), as part of its program on Nondestructive Testing, managed by Dr. J. Conrad Trulson, Deputy Director for Materials Sciences. The work was administered by the Naval Air Engineering Center (NAEC), under Contract No. N00156-71-C-0550, with Mr. Forrest S. Williams serving as Technical Manager.

This final annual technical report covers the period from 1970 October 5 to 1971 November 5 in the three-year program at Avco/SD. Mr. J.R. Zurbrick was Project Manager for the first 9 months of this year's effort. Upon Mr. Zurbrick's termination, Mr. E.A. Proudfoot was appointed Project Manager for the next two months and Mr. C.H. Hastings for the remainder of the program covering final report preparation.

We gratefully acknowledge the generous assistance of Mr. A.M. Chetson, Mr. A. Hauze, and Mr. Edward Janas in the laboratory measurement phases, and of Mr. D.R. Smith in the preparation of the adhesive bond test specimens.

## ABSTRACT

The third annual period of research and development at Avco Systems Division into Nondestructive Tests for the Evaluation of Bonded Materials, sponsored by the Advanced Research Projects Agency, has continued the course set by the first and second year's studies, namely development of NDT techniques for characterizing metallic substrate surfaces.

Continued studies of the relative influence of parametric variables on bond strength has shown the overriding influence of surface free energy ($\gamma_s$) as compared with contact angle on prepared substrates. The effective strain value ($k_o$) was found to be very complex. Its empirical treatment as if it consists only of uniformly distributed axial strain is a possibly useful solution which permits linking bond strength primarily to surface free energies.

Also, during this third year, effort was devoted to development of nondestructive, optical, and spectrophotometric techniques for characterizing contaminants which frequently occur on substrate surfaces. Although the most sensitive techniques available were employed, they did not reveal correlations with bond strength variability observed.

## TABLE OF CONTENTS


FOREWORD . . . . . .ii

ABSTRACT . . . . . .iii/iv

I. INTRODUCTION . . . . . .1

II. SUMMARY . . . . . 3

III. PROGRAM PLAN . . . . . .5

IV. SURFACE CHARACTERIZATION - THEORY . . . . . 11

V. SURFACE CHARACTERIZATION - EXPERIMENTAL . . . . . 20

A. Materials . . . . . 20
B. Substrate Surface Preparation and Evaluation . . . . . .20
C. Specimen Surface Preparation and Evaluation . . . . . 30
D. Adhesive Bonding . . . . . .41
E. Evaluation of Bonded Specimens . . . . . .41
F. Tensile Testing . . . . . 48
G. Correlations . . . . . .48

REFERENCES . . . . . .52

APPENDIX I - Surface Cleaning Treatments

## ILLUSTRATIONS


| | | |
|---|---|---|
| Figure 1 | Illustration of Energy Concept in the Predictive Equation for Bond Adhesive Strength | 12 |
| Figure 2 | Influence of Substrate Surface Free Energy on Bond Adhesive Strength; All Other Variables Held Constant | 14 |
| Figure 3 | Influence of Contact Angle on Bond Adhesive Strength; All Other Variables Held Constant | 15 |
| Figure 4 | Calculation of Contact Angle Cosine As Function of Normalized Liquid Droplet Height | 25 |
| Figure 5 | Calculation of Contact Angle As a Function of Normalized Liquid Droplet Neight | 26 |
| Figure 6 | Light Reflection Technique Using a Photovolt Glossmeter | 27 |
| Figure 7 | Light Reflection Using a Helium-Neon Laser Source and Separate Light Energy Detector | 28 |
| Figure 8 | Horizontal Scan with 1/8" Vertical Index on Stainless Steel Plate S-4 Using the Red Laser Light Reflection Technique | 31 |
| Figure 9 | Photograph of Plate S-4 for Comparison with Scan Information (purposely inverted) | 32 |
| Figure 10 | Horizontal Scan with $\frac{1}{4}$" Vertical Index on Aluminum Plate A-3 Using the Red Laser Reflection Technique | 33 |
| Figure 11 | Horizontal Scan with $\frac{1}{4}$" Vertical Index on Titanium Plate T-14 (circular lathe-turned pattern) | 34 |
| Figure 12 | Typical Specimen Layout for Aluminum 6" x 6" x 1/8" Plate | 35 |
| Figure 13 | Adhesive Bond Specimen | 36 |
| Figure 14 | Beckman DK-2 Ratio Recording Spectrophotometer | 38 |
| Figure 15 | Monochromatic Detection Light Path | 42 |
| Figure 16 | Total Reflectance Arrangement in Sphere | 43 |
| Figure 17 | IR Total Reflectance for Various Contaminants | 44 |
| Figure 18 | IR Total Reflectance; Specimen AlA - Clean Aluminum | 45 |

## ILLUSTRATIONS cont.


Figure 19 IR Total Reflectance; Specimen A1D - Finger Print on Aluminum . . . . . 46

Figure 20 IR Total Reflectance; Specimen A1G - Floor Dust on Aluminum . . . . . 47


## TABLES


Table I Surface Roughness - Aluminum 6061-T6 . . . . . 21

Table II Surface Roughness - Titanium Ti-6Al-4V . . . . . 22

Table III Surface Roughness - Stainless Steel 17-7 PH . . . . . 23

Table IV Comparison of Light Reflection Techniques . . . . . 29

Table V Contamination Procedures . . . . . 37

Table VI Beckman Recording Spectrophotometer Specifications . . 39

Table VII Summarizing Modes of Operation . . . . . 40

Table VIII Thickness - Bonded Specimens . . . . . 49

Table IX Tensile Bond Test Results . . . . . 50

# I. INTRODUCTION

The practical application of adhesive bonded structures in military hardware designs over the past decade created a need for means to assure bond quality. Nondestructive instrumentation and techniques were correspondingly developed to detect bond/unbond in most situations and predict bond cohesive strength in certain restricted cases, mainly honeycomb sandwich structures. Confidence in adhesive bonding for primary load bearing structural components has grown to the point where current and anticipated designs present a critical need for nondestructive means to predict adhesive bond strength in production floor and field service applications.

Review during the first year of the subject contract of the problem as a whole, and subsequent subdivision into the contributing parts revealed that currently available tests and controls for materials and processing are seldom applied in practice to the extent necessary for proper control[1].

Discussions with experienced adhesives engineers revealed service failures attributable to lack of testing/controls in nearly every category listed in an idealized bonding sequence. Obviously the reason for exclusion of many tests and control steps was economic in nature. Highly reliable adhesive bonds cannot be assured when any critical control or test is eliminated.

The most critical area for NDT research and development was concluded to be that of substrate surface preparation prior to bonding. Today, adherend surfaces are not specifically controlled, but are accepted on the basis of controls applied to the processes by which they are produced. As a consequence, an extensive Surface Condition Study was conducted to learn the influences of surface roughness, contact angle, and mechanical means of preparation on adhesive bond strength.

In order to develop nondestructive tests responsive to surface characteristics, we first identified those characteristics which in turn are important to adhesive bonding. The science of adhesion offered a few solid clues, but not a firm and complete foundation. Adhesive bonding technology offered many empirical rules and an almost equal number of exceptions.

Much of the science of adhesion literature deals with the properties of free surfaces with extrapolations into resultant interfaces. More detailed searching led us rapidly into the physical chemistry and thermodynamics of free surfaces where lubrication, surfactants, friction phenomena, and catalysis enter the picture. The result of these investigations has been the predominance of the "work of adhesion" term and the wide use of surface free energies as derived from contact angle measurements to explain various observed phenomena in each area of industrial specialty. For the most part, and from necessity, such work deals with ideal conditions; however, sufficient attention has been given departures from the ideal to offer guidance in explaining those "interfacial" failures that do occur in spite of such an occurrence being theoretically unlikely.

The second year's work was devoted to a combined experimental and theoretical program directed at the development of a quantitative bond strength prediction capability based on nondestructively measurable parameters. While a practical solution has not been attained, some important observations resulted from this work and point the way for further investigations. Among these observations are the following:

1. Substrate surface free energy is influenced by the mechanical means used to generate the surface.

2. The preponderance of energy dissipated in the breaking of a "good" rigid bond is dissipated in the bulk of the adhesive and adherends, and by comparison, the energy required to create new surfaces is very small.

3. At least for the cases studied under this contract, failure of adhesively bonded butt tensile and core shear specimens usually initiates at or near the substrate-adhesive interface, and the bond strength is roughly inversely proportional to the area of the interfacial separation.

4. A strong preliminary correlation was found to exist between aluminum substrate surface free energy, calculated from experimental data, and white light specular reflectance.

The initial portion of the current year's work was devoted to further analysis of the predictive equation proposed as a result of the second year's work, and is due primarily to J.R. Zurbrick. The second portion of the current year's work was directed toward further refinement of light reflectance techniques; visible "white" light and laser experimentation being carried on by J.R. Zurbrick; and spectrophotometric reflectance investigation in the ultraviolet, visible and infra-red regions being done by E.A. Proudfoot.

## II. SUMMARY

The current year's work (1970 October 5 - 1971 November 5) included two related investigations:

1. Analysis and further development of the proposed predictive equation, and

2. Exploration of light reflectance as a means to characterize surfaces.

The predictive equation proposed by J.R. Zurbrick has been helpful in increasing our understanding of adhesive bonding, but fails in several respects to adequately describe adhesive bond strength. Some of the more important shortcomings of the equation are:

1. It fails to account for the presence of weak interlayers, possibly the most important source of adhesive type failures.

2. It assumes that all of the energy dissipated in the creation of new surface is dissipated at the interface; our own observations indicate that part of this energy is consumed at the interface, and part consumed by cohesive failure.

3. The energy term (numerator) may be incorrect (from the practical point of view, this would not be too important, since this quantity is derived from experimental data).

4. The equation cannot account for minute local unbonded regions that play an important role in fracture as stress risers.

5. The strain term is very difficult to handle experimentally, since the vast majority of measured strain is not in the bond line; further, the strain in the bond line is complex.

The observation in the previous year's work of a gross correlation between specular white light reflectance and bond strength led to a further investigation of reflectance of electromagnetic waves in and near the visible part of the spectrum. Topographic mapping techniques were experimentally explored with white light and with a helium-neon laser. Near ultraviolet, visible, and near infra-red spectrophotometry measurements were performed on purposely contaminated specimens. The spectrophotometry was done in order to determine if existing equipment could detect harmful contamination existing at levels that are not readily visually observable.

Disappointingly, none of the optical techniques employed seemed to respond to the deliberately introduced surface contaminants. At the same time, examination of tensile results and fractured surfaces showed that the contaminants had, in fact, produced a range of values and fracture types. Although preliminary tests using UV spectrophotometry showed absorption peaks due to gross contamination, sensitivity proved to be inadequate at lower levels of contamination capable of producing weak, adhesive-type failures.

## Conclusions and Recommendations

It is concluded that:

1. Substrate surface free energy appears to be an overriding variable controlling bond strength.

2. A gross relationship exists between substrate surface free energy and white light or coherent laser reflectance. The reflectance measurements respond to variations in mechanical surface preparation techniques. Surface roughness, itself, does not appear to be a primary influencing variable on bond strength or on surface free energy.

3. The addition of normal types and amounts of contamination was not observable using the ultraviolet and infra-red spectrophotometric techniques available. However, the contaminants did produce weakened and adhesive-type failures.

It is recommended that:

1. Effort be continued to develop nondestructive techniques for characterizing substrate surface free energy as influenced by

   a. Mechanical finishing methods,
   b. Typical contaminants, and
   c. Surface preparation procedures.

2. Refining the equation developed by J.R. Zurbrick in an effort to relate surface free energy to adhesive bond strength, as influenced by other process variables.

## III. PROGRAM PLAN

### 1. Aims and Goals

The long-term goal of this program has been to significantly advance technological capabilities to control the adhesive bonding process and thereby, the resultant adhesive bonds.

The past year's program was aimed toward developing nondestructive test methods and techniques for characterizing the adhesive bond strength-controlling parameters of typical metallic substrate surfaces used in aircraft fabrication, based on a recently developed relationship for predicting bond adhesive strength.[2] The equation states:

$$BAS = \frac{\gamma_S - \gamma_L \cos\theta}{(\frac{1}{2})(k_o)(d)(175127)} \qquad (1)$$

where: BAS = bond adhesive strength, lbs/in$^2$

$\gamma_S$ = substrate surface free energy, ergs/cm$^2$

$\gamma_L$ = liquid surface free energy, ergs/cm$^2$

$\theta$ = contact angle, degrees

$k_o$ = effective strain

d = bondline thickness, inch

Bond adhesive strength is the load per unit cross-sectional area resulting from a failure at the adhesive/substrate interface, where the mode of failure is a brittle fracture followed by shock-wave cleavage propagation. This is distinguished from bond cohesive strength (BCS) resulting from a failure within the adhesive material, where the mode of failure is a viscoelastic rendering, tearing, or peeling.

In using equation (1), nondestructive means are necessary to determine $\gamma_S$, $\theta$, and d, when $k_o$ and $\gamma_L$ are known for a given joint configuration and reference liquid. The $(\frac{1}{2})$ is the unit integral of a linear stress strain curve, the most simple case. The proper unit integral function must also be known for a given adhesive bond system. This well-defined problem serves to pinpoint test development goals.

### 2. Detailed Outline

PHASE I. Surface Characterization - Theory

A. Expansion of Predictive Equation

1. Analysis for theoretical soundness in terms of "ground state".

2. Study of the factors which may be included in "apparent strain" ($k_o$).

3. Determination of the exact influence of each factor in the relationship, both in terms of energy and practical engineering properties.

B. Adhesive Strength/Cohesive Strength Concept

1. Adhesive strength-energy relationships associated with shock-wave propagation as the mode of failure (brittle fracture) at or near the substrate-adhesive interface.

2. Cohesive strength - energy relationships associated with viscoelastic peeling or tearing as the mode of failure within the adhesive material.

3. Interrelationships or interactions between adhesive failure and cohesive failure (slip-stick) strain-rate sensitivity, temperature dependence.

4. Theoretical foundations based on quantum mechanics of chemical bonding.

C. Material-Energy Interaction Links

1. Light reflection from the substrate surface.

2. Ultrasound transmission through a surface from the substrate phase into the gas phase.

3. Liquid surface free energy comparison between distilled water and an adhesive formulation.

4. Surface free energy changes associated with setting of an adhesive; conversion from liquid to solid.

5. Low frequency electric field reflection from a metallic substrate surface.

PHASE II . Surface Characterization - Experiment

A. Materials

1. Substrates to be evaluated

a. Aluminum Alloy 6061-T6
4 square feet, 1/8 inch thick sheet

b. Titanium Alloy Ti-6Al-4V (annealed)
4 square feet, 1/8 inch thick sheet

c. Stainless Steel Alloy 17-7PH
4 square feet, 1/8 inch thick sheet

2. Adhesive Systems

a. Epoxy formulation, Epon 828/DETA

b. Unsupported film-epoxy
FM-97U

c. Paste - Polyimide
Pyralin 4707

3. Surface preparation compounds

a. Aluminum Alloy - sulfuric acid sodium dichromate etch solution.

b. Titanium Alloy - Pasa-Jell 107/C (for immersion solutions) or Pasa-Jell 107M (for non-immersion technique).

c. Stainless Steel Alloy - perchloroethylene solvent rinse.

4. Test specimen auxiliary materials

a. Pull-bars - 3/4 inch diameter aluminum alloy 6061-T6

b. Reverse-loading fixture - low carbon steel

B. Evaluation Prior to Adhesive Bonding

1. Substrate Test Plates

a. Cut 6" x 6", 16 per substrate alloy

b. Surface regeneration on one side of each plate to provide a variety of roughnesses and lays using various machining, grinding, and grit-blasting techniques.

2. Identification Grid Overlay

a. 1 inch by 1 inch grid identification system separate from plates.

b. Frame with taut-wire construction.

3. Surface Condition Characterization

a. Roughness and lay

b. Water-break test with distilled water

c. Contact angle with distilled water

d. Nondestructive tests for substrate surface free energy

1. Specular white light reflection

2. Ultrasonic gas-phase transmission

3. Laser reflection

4. Electric field reflection

e. Photographic records

C. Adhesive Bonding

1. Surface cleaning and preparation

2. Water-break test

3. Contact angle tests

4. Nondestructive tests

5. Photographic records

6. Adhesive preparation and application

7. Substrate position fixturing

8. Adhesive bond curing and bondline trim

D. Evaluation Following Adhesive Bonding

1. Bondline thickness measurement

a. Micrometer

b. Ultrasonic caliper technique

2. Mechanical test for ultimate bond strength and total extension.

3. Inspection and photographic record of failure zones.

E. Data Correlation and Analysis

1. Comparison of water-break observations and contact angle cosine values for area agreement.

2. Bondline thickness values by micrometer and ultrasonic caliper.

3. Predictive equation analysis of experimental data.

4. Correlation between nondestructive substrate surface response values and calculated values of substrate surface free energies.

5. Comparison of measured strains with $k_o$ values and its factors.

PHASE III. Nondestructive Test Methods Development

A. Light Reflection

1. Light sources

a. White light source
Photovolt glossmeter optics

b. Incoherent monochromatic light
Sodium vapor or filter monochromators

c. Coherent monochromatic light
Helium-neon laser source

2. Types of energy change

a. Specular reflection; general attenuation due to diffuse scattering

b. Spectral reflectance; frequency dispersion

3. Measurement instrumentation

a. Photovolt glossmeter, photocells in a balanced bridge network

b. Incident angle goniometer

c. Optical spectrometer

d. Light intensity meter

e. Laser power meter

B. Ultrasonic Gas-Phase Transmission

1. Acoustic sources and receivers

a. Narrow band, high gain transducers 0.5 to 10.0 MHz

b. Wide band, low damped transducers 0.2 to 1.0 MHz

2. Types of energy change

a. Selected frequency attenuation

b. Selected frequency generation

3. Measurement instrumentation

a. Coupling medium fixture

b. Receiver fixture

c. Oscilloscope/spectrum analyzer

C. Electric Field Reflectometry

1. Electric field sources and receivers

a. Specially-designed, small area dielectric probes, coplanar

b. Parallel plate probe

2. Types of energy change

   a. Relative phase shift, giving a capacitance value at bridge balance.

   b. Relative attenuation, giving a dissipation factor value at bridge balance.

3. Measurement instrumentation

   a. Automatic capacitance bridge, 1 kHz

   b. Capacitance bridge assembly, highest sensitivity, 100 Hz to 500 kHz frequency range.

D. Contact Angle

1. General design approaches

   a. Electromechanical based on force equilibrium of contained droplet.

   b. Electro-optical based on free droplet equilibrium.

2. Test requirements

   a. Rapid and convenient

   b. Does not contaminate surface

   c. Direct correlation between optical contact angle reading and instrumentation indication

   d. High accuracy and reproducibility

## IV. SURFACE CHARACTERIZATION - THEORY

### Predictive Equation Analysis

#### 1. Illustration of basic assumption

The predictive equation serving to guide research in this program is based on the assumption that bond adhesive strength and interfacial surfaces free energy ($\gamma_{SL}$) are one-and-the-same. The terms in the equation resulted from the process of converting bond strength engineering units to the units and concepts of surface energetics. The basic assumption is illustrated in Figure 1. Here the Thomas Young equation is pictured in terms of specific stored energy levels relative to a generalized "ground" (highest energy) state. The viewpoint is from that of the substrate, which usually is the material capable of highest stored energy and therefore the dominate force in establishing an adhesive bond.

Just prior to wetting, the substrate surface, in air, is at its highest stored energy level. (If surrounded by vacuum, that surface would essentially be at the ground state.) At the moment of wetting, work is performed by the stored substrate surface energy on the contacting liquid to pull it over the substrate surface, thereby effecting the "bonded state" energy level, an energy change equal to ($\gamma_S$). Immediate and subsequent needs for energy to complete chemical bonds at the interface, or during cure within the adhesive, are supplied by thermal transfers within and among the bulk materials involved, as derived from heat and pressure provided during bond fabrication.

Breaking the bond at the interface either slowly or rapidly raises the energy of the interface to the intermediate "broken bond state" energy level, an energy change equal to ($\gamma_{SL}$). Intuitively, this may be considered to be a "dirty" surface, being coated with essentially a monolayer of the cured adhesive. Should the original wetting liquid be placed on this surface, wetting would be minimal. The substrate must therefore be "cleaned" to raise it again to a satisfactorily bondable "wetting state", an energy change equal to ($\gamma_L \cos \theta$).

#### 2. Selected relationships

By fixing all but one of the six independent variables in the predictive equation, the remaining variable may be evaluated for its singular influence on bond adhesive strength. A large number of calculations were made covering these ranges of values:

| | |
|---|---|
| substrate surface free energy, $\gamma_S$ | 70-400 ergs/cm$^2$ |
| contact angle, $\theta$ | 0° - 90° |
| bondline thickness, d | 0.0005 - 0.050 inch |
| liquid surface free energy, $\gamma_L$ | 20-100 ergs/cm$^2$ |
| effective strain, $k_o$ | 0.00005 - 0.0004 |
| stress strain integral, $\int(\sigma, \epsilon)$ | 0.2 - 0.5 |

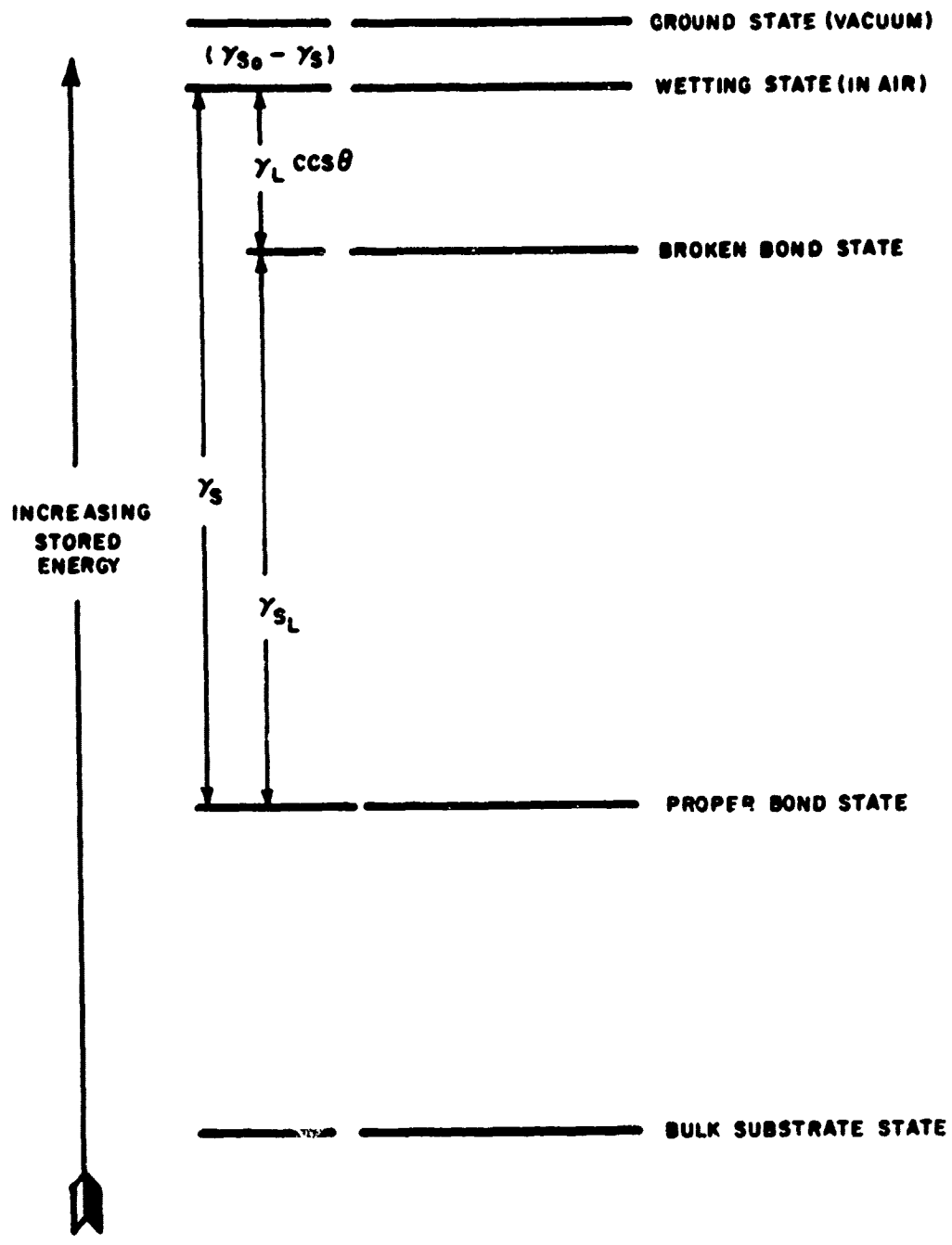


Figure 1 ILLUSTRATION OF ENERGY CONCEPT IN THE PREDICTIVE EQUATION FOR BOND ADHESIVE STRENGTH.

Of these, substrate surface free energy and contact angle were studied in greatest detail. In Figures 2 and 3, values for the parameters were selected from prior experience with butt tensile specimens. The dramatic, linear effect of $\gamma_S$ on bond adhesive strength is apparent. The range of ($\gamma_S$) values between the dashed lines has been observed by others to be that typical for substrate metals in the solid state[3].

The contact angle contribution is much less dramatic over the range useful for adhesive bonding, roughly $0^o$ to $30^o$. Bond strength increases with increasing contact angle (all else held constant), which is quite opposite to popular beliefs in the literature. There is no real conflict, however, when it is remembered that a small increase in substrate surface free energy will have a large inverse influence on contact angle. Thus small contact angles are indicative of properly prepared, nigh-energy substrate surfaces. A high contact angle is usually accompanied by poor wetting. Should coverage be spotty, the calculated bond adhesive strength would then be reduced by the fraction of area actually bonded.

3. Effective strain factors

The numerical values of effective strain ($k_o$) calculated from experimental data were found to be 10 to 100 times smaller than expected. This situation resulted from the fact that in actuality not all of the stored energy is converted to generating the new surfaces at the moment of fracture[4]. The remainder is dissipated in work hardening the new surface, bulk material changes, and vibratory losses in the substrates and testing machine. Most important here has been the assignment of the resultant discrepancy to effective strain where it properly belongs, rather than to the surface free energy terms which are known to range between 100 and 300 ergs/cm$^2$.

The individual strain contributions to $k_o$ suggest from the layered nature of an adhesive joint that an arithmetic or additive approach be taken, rather than a geometric or product interrelationship. The distribution of energy and corresponding axial deflections under the load at the moment of fracture are such that the interfacial contribution is largely masked by the huge energy and deflection quantities operating elsewhere. An example will clarify that statement:

Using the butt tensile specimen and typically average values gained from the previous year's work, we can calculate the energy used to form the new surfaces at failure:

$$\text{energy} = (\tfrac{1}{2})\ (\text{BAS})\ (\epsilon)\ (d)\ (A)\ (1129849)\ \text{ergs}$$

where: BAS = bond adhesive strength, psi

$\epsilon$ = axial strain in tension

d = bondline thickness, inch

A = bonded area of specimen, inch$^2$

$(\tfrac{1}{2})$ = integral of stress and strain to failure

$$\text{energy}_I = (\tfrac{1}{2})\ (5000)\ (0.00005)\ (0.006)\ (0.750)^2\ (\tfrac{\pi}{4})\ (1129849)$$

$$\text{energy}_I = 374\ \text{ergs}$$

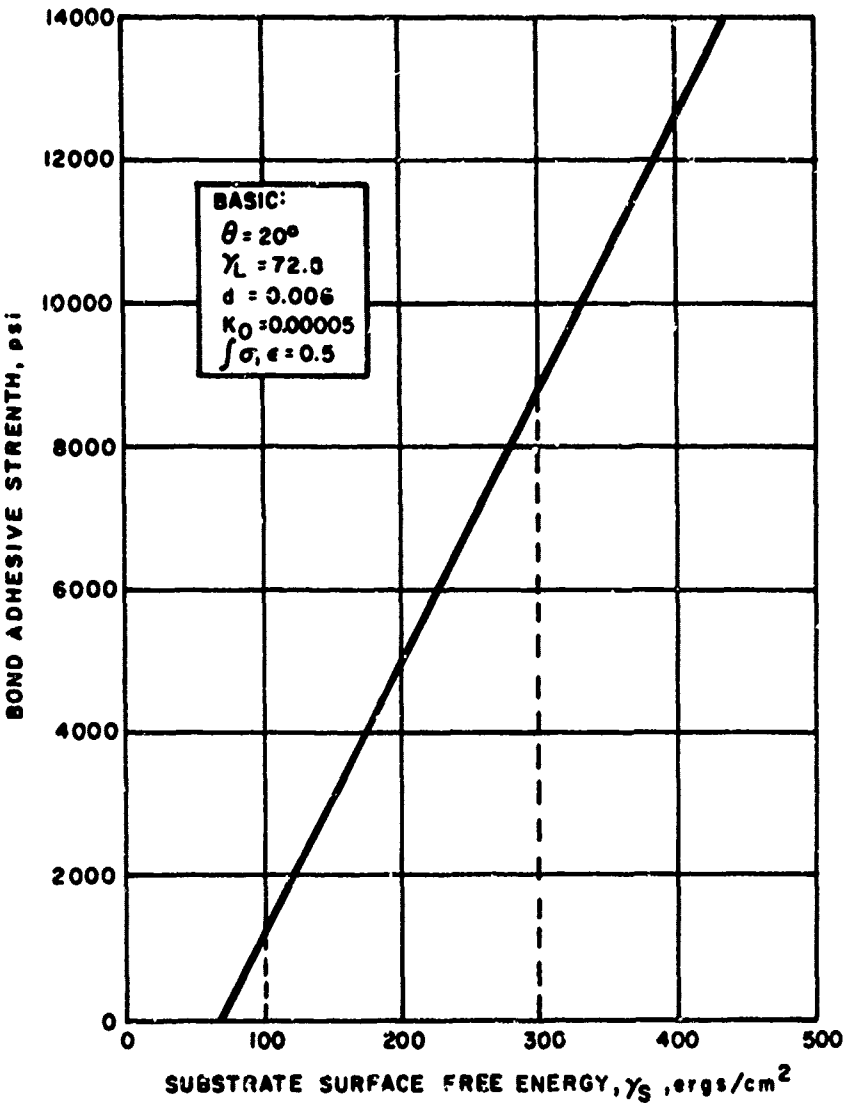


Figure 2 INFLUENCE OF SUBSTRATE SURFACE FREE ENERGY ON BOND ADHESIVE STRENGTH, ALL OTHER VARIABLES HELD CONSTANT.

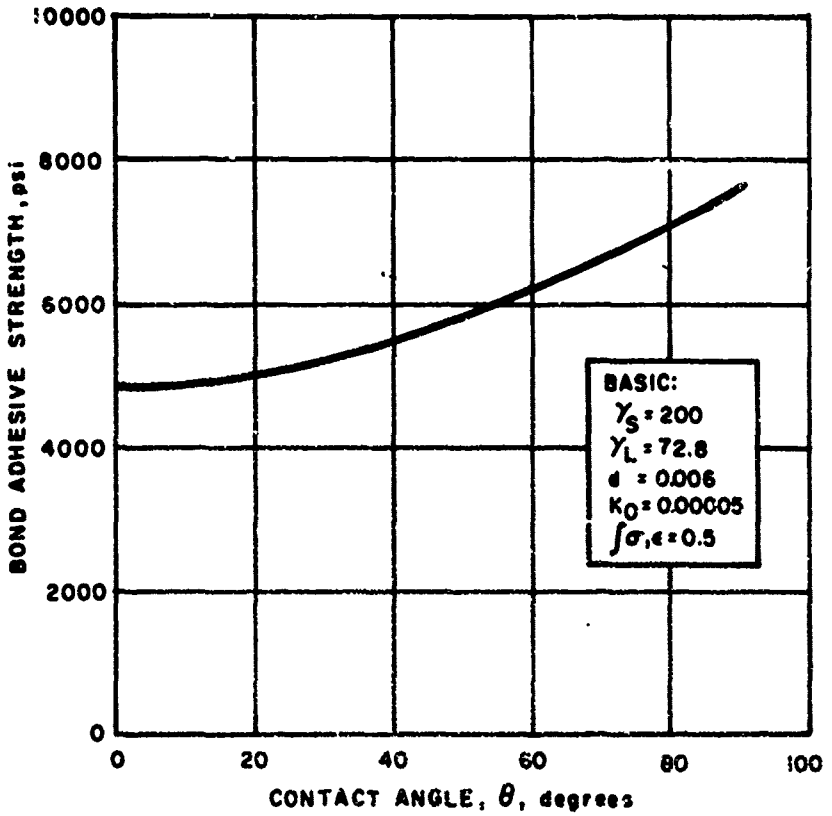


Figure 3 INFLUENCE OF CONTACT ANGLE ON BOND ADHESIVE STRENGTH, ALL OTHER VARIABLES HELD CONSTANT.

Energy stored and then dissipated in the substrates is:

$$\text{energy}_S = (\tfrac{1}{2})\ (5000)\ (0.00050)\ (4.0)\ (0.750)^2\ (\tfrac{\pi}{4})\ (1129849)$$

$$\text{energy}_S = 2{,}496{,}000 \text{ ergs}$$

Energy stored and then dissipated in the adhesive layer:

$$\text{energy}_A = (\tfrac{1}{2})\ (5000)\ (0.01000)\ (0.006)\ (0.750)^2\ (\tfrac{\pi}{4})\ (1129849)$$

$$\text{energy}_A = 74{,}873 \text{ ergs}$$

$$\text{energy total} = 2{,}571{,}250 \text{ ergs}$$

Similarly for axial extension:

$$\Delta_d = \frac{(BAS)}{E}\ (d)$$

where E = modulus of elasticity of bulk material, substrate or adhesive.

$$\Delta_{d_S} = \frac{5000}{10 \times 10^6}\ (4.0) = 0.002"$$

$$\Delta_{d_A} = \frac{5000}{0.5 \times 10^6}\ (0.006) = 0.00006" = 60\ \mu \text{ inch}$$

and for comparison, the value previously reported:

$$\Delta_{d_o} = (0.00005)\ (0.006) = 0.3\ \mu \text{ inch}$$

These figures show the predominant influence of the substrates in the mechanical test. This sort of analysis, however, uses the gross simplification of axial strain, which is not the actual case in the adhesive bulk or the interface at all. There the forces are shear and tension perpendicular to the axis, being greatest at the bondline edges. The proper micromechanical analysis would resolve these forces for suitable accounting, but the mathematics necessary for practical bond strength predictions would be formidable. What has been learned is that the forces and areas can be arbitrarily treated as if only uniformly distributed axial stresses exist, and the effective strain value ($k_o$) used to empirically characterize the test specimen or bonded joint configuration. By this simple and straightforward means we can link practical adhesive bond strength to the operating surface free energies. The otherwise overpowering effects of substrates and bulk adhesive are thereby eliminated.

In previous work under this contract, it has been shown:

1. Substrate free energy to be influenced by the mechanical means used to generate the surface.

2. The preponderance of energy dissipated in the breaking of a "good" rigid bond is dissipated in the bulk of the adhesive and adherends,

and by comparison, the energy required to create new surfaces is very small.

3. At least for the cases studied under this contract, failure of adhesively bonded butt tensile and core shear specimens usually initiates at or near the substrate-adhesive interface, and the bond strength is roughly inversely proportional to the area of the interfacial separation.

4. A gross correlation exists between the white light specular reflectance, measured prior to bonding and the breaking strength of the bonds tested in this program.

Based on experimental and theoretical work found in the literature concerned with adhesive bonding, results 1 and 2 above are to be expected. Result number 3, however, was rather surprising, and has been the subject of considerable thought and discussion. It has been concluded that this result is surprising primarily due to (a) the usual method of reporting adhesive fractures; i.e., these would be reported as cohesive fractures, or at best, 97 percent cohesive, 3 percent adhesive, and (b) an over simple interpretation of bonding theory, which correctly implies that interfacial bonds are so strong that only cohesive failures are likely, without regard for cohesive failures in interlayers of tens of angstroms thickness, and the possibility of stress risers in the form of unwetted areas or surface asperities with micron dimensions. Result number 4 may combine with result number 3 in such a way as to indicate an area of investigation that will eventually lead to a positive means to assure a substrate's readiness for bonding. To demonstrate the validity of the proposed approach, a brief review of some of the factors already known about adhesive bonding is necessary.

There exists a multitude of theoretical studies, based primarily on the Thomas-Young wetting equilibrium equation and on Dupre's and Harkins work of adhesion equations, indicating that once a material comes into intimate contact with another material on a molecular scale (wets), very strong bonds will be formed. In the case of structural adhesives, these interfacial (on a molecular scale) bonds will be at least an order of magnitude stronger than the cohesive strength of the adhesive. This is true when only van der Waal's forces are operating; polar materials, or hydrogen bonding materials, will produce even stronger interfacial bonds.[5]

There are at least 4 reasons why "interfacial" failures are experienced. (Interfacial, as used here, is on a macroscale and refers to failures occurring at or near the interface). These may be listed as:

1. incomplete wetting
2. stress risers at the interface
3. weak interlayers
4. residual stress

Incomplete wetting can arise from at least two causes. First, the processing cycle may be such that the adhesive does not have time to flow into all of the crevices and cavities of the surface before hardening of the adhesive occurs.[6] Second, local regions on the surface may have an energy state not conducive to wetting, i.e., the adhesive will not flow over and bond to regions having lower free energy than the surface tension of the adhesive.

Regardless of the origin of such regions, microscopic or even submicroscopic voids tend to dilate rapidly under tensile stress and reveal failures of interfacial origin upon fracture. Obviously, the adhesive-adherend system and the processing cycle must be chosen such that sufficient time is available for complete wetting, and the surfaces must have the proper free energy on the submicroscopic level if this type of failure is to be avoided.

Stress risers may occur as a result of entrapped air of other non-wetted regions as described in the preceding paragraph or may be a result of surface topography on the micron scale. Since ideal surface topography on the microscopic scale is a trade-off between several desirable and undesirable factors, most of which are not well understood (clean surface, large area surface, highly reactive surface, crack stopping ability, stress concentration), it appears that one must concentrate on the complete wetting of the surface to reduce stress concentration from unbonded regions, and for the time being, live with stress concentration from surface asperities.

The third reason listed for "interfacial" failures seems likely to be the most prevalent. Except for laboratory experiments and rare special cases, adhesive bonding is never carried out with atomically clean surfaces. Surface conditioning prior to bonding is always such as to produce a highly reactive surface. Such surfaces naturally tend to lower their energy by interaction with whatever environment is available. Immediately on exposure to the atmosphere this surface adsorbs oxygen and nitrogen, and forms strong polar or hydrogen bonds with water vapor or vapors from cleaning agents, etc. Further, metallic surfaces, in particular, form oxides which are strongly chemically bonded to the adherend surface. These oxide layers, consisting mainly of polarized oxygen groups, are usually highly desirable surfaces for adhesive bonding. Adhesive bonding, then, does not usually depend on attachment of the adhesive to the base metal surface; instead the bond is formed between the adhesive and some interlayer of oxides and adsorbed molecules. These oxides and adsorbed molecules are in turn firmly attached to each other and to the adherend. As long as these adsorbed molecular gas layers and oxide layers are thin, they possess good strength, and this strength depends on van der Waal's forces (including the quantum mechanical "dispersion" forces) and in many cases polar and hydrogen bonding as well. Weak "interfacial" bonding occurs when these layers become too thick and the strength of the composite system depends too strongly on the cohesive strength of the gas or oxide layer. Just what is meant by "too thick" is not very well known, but is almost certainly considerably less than 100 Å; this thickness also probably varies somewhat with the layer material, but in all cases is quite small (oxides which are permeable to the adhesive are an exception and may be much thicker, however). A "clean" surface, then, is a rather relative thing, and really only implies a surface suitable for producing strong adhesive bonds to strongly bonded strong interlayers. This "clean" surface must be hydrophilic to promote wetting, it must have a surface topography that permits complete wetting by the adhesive used, it may have to possess certain undefined chemical properties, it may have to carry ions adsorbed from the cleaning bath, and it may have to develop a polarized or polarizable coating; above all, it should be reproducible. Assuming surface topography at the sub-micron level can be controlled by mechanical abrasion and/or chemical treatment, all the other factors are controlled by the chemical nature and thickness of the various materials on the surface. It is here suggested that future effort be concentrated in the direction of providing means of identifying the nature of these interlayers and hopefully suggesting ways of measuring their thickness. This is not

really a new approach; the volta potential work of Matting[7], based on electron emission and designed to measure the work function of a surface would be influenced by interlayers; infrared analysis has been investigated with limited success by Johnson[8], X-ray fluorescence has been used to identify foreign matter, and Huntsberger[9] has made reflectance thickness measurements in the visible wavelength regions. It is deemed likely that the white light reflectance measurements made by Zurbrick[10], and found to correlate grossly with bond strength, were influenced by the presence of surface contaminants as well as by surface roughness.

## V. SURFACE CHARACTERIZATION - EXPERIMENTAL

### A. Materials

Three materials in the form of 1/8" thick plate stock were fabricated into 6" x 6" specimens for the NDT surface characterization study: aluminum 6061-T6, titanium 6Al-4V, and stainless steel 17-7PH.

### B. Substrate Surface Preparation and Evaluation

Each of 16 plates for the three metal substrates was prepared on one surface by various machining, grinding, and grit blasting methods. Roughness data are summarized in Tables I, II, and III. In addition to contact angle measurement technique development, each plate was evaluated nondestructively using a white light reflection technique and a helium-neon laser red light reflection technique.

#### 1. Contact angle measurement development

Continuation of efforts to design a high resolution manometer for droplet pressure measurement was carried as far as obtaining a transducer head and associated electronics. Various approaches to estimating droplet pressure values gave a range of 2 to 600 microns Hg differential pressure as a function of contact angle ($\theta$) from $0^{o}$ to $90^{o}$ for typical droplet sizes. This extremely small pressure differential must "ride" on top of ambient barometric changes, requiring a matched, separate transducer for compensation. The advantage of this technique is that it supplies a single integrated or representative average value. Mechanics of sampling the droplet internal pressure without significantly disturbing the droplet, as well as adding or subtracting liquid while finding maximum and minimum contact angles were studied. It became evident that just the practical mechanics of this technique would render it cumbersome and tedious. A more direct and simple approach was sought.

Preliminary designs for a small optical device which essentially performs the Langmuir angulation were studied. Again the mechanics of liquid addition or subtraction cause interference, but the major problem is the accurate location of the three-phase contact point preliminary to making a measurement. This technique would require a number of measurements on each drop to obtain the representative average value.

While performing the analytical studies it was necessary to link droplet dimensions and shape to contact angle. The first approximation was to assume that the droplet is always a spherical segment of some sphere which varies in size (radius).

The following relationships are then evident:

$$V_{ss} = \left(\frac{\pi}{6}\right) (h) (h^2 + 3 x^2) \qquad (1)$$

and,

## TABLE I

## Aluminum 6061-T6

## Surface Roughness

| Specimen | Surface Preparation | Nominal Roughness | Measured Roughness | | |
|---|---|---|---|---|---|
| | | | Profilometer rms | Tally CLA | Surf rms |
| A-1 | CGHP | ≈45 | ≈150 | 105 | 115.5 |
| 2 | FGHP | ≈48 | 30-40 | 35 | 38.5 |
| 3 | Grinding | 16 | 5-45 | 13 | 14.3 |
| 4 | Wire Brush | 32 | | $39^{S}$ - $68^{D}$ | 42.9 - 74 |
| 5 | Wire Brush | 64 | | $30^{S}$ - $70^{D}$ | 33-77 |
| 6 | Milling | 16 | | 37 | 40.7 |
| 7 | Sand Paper | 16 | | 15 | 16.5 |
| 8 | Sand Paper | 32 | | 28-36 | 30.8-39.6 |
| 9 | Milling | 32 | | 34 | 37.4 |
| 10 | Milling | 64 | | 40 | 44 |
| 11 | Turning | 16 | 5-40 | 21 | 23.1 |
| 12 | Turning | 32 | 25-35 | 23 | 25.3 |
| 13 | Turning | 64 | 50-70 | 40 | 44 |
| 14 | Turning | 128 | 120-145 | 100 | 110 |
| 15 | Lapping | 4 | | | |
| 16 | as rec'd | - | | 12 | 13.2 |

NOTE: Center Line Average (CLA) ⟶ 1.1 CLA = rms

## TABLE II

## Titanium Ti-6Al-4V

## Surface Roughness

| Specimen | Surface Preparation | Nominal Roughness | Measured Roughness | | |
|---|---|---|---|---|---|
| | | | Profilometer rms | Tally CLA | Surf rms |
| T-1 | CGHP | ≈45 | 75-100 | 82 | 90.2 |
| 2 | FGHP | ≈48 | 22-28 | 24 | 26.4 |
| 3 | Grinding | 16 | 16-18 | 16 | 17.6 |
| 4 | Grinding | 32 | 25-40 | 20-30 | 22-33 |
| 5 | Grinding | 64 | 60-80 | 29-60 | 31.9-66 |
| 6 | Milling | 16 | | 160 | 176 |
| 7 | Sand Paper | 16 | | 4.5 | 4.95 |
| 8 | Sand Paper | 32 | | | |
| 9 | Milling | 32 | | 29 | 31.9 |
| 10 | Milling | 64 | | | |
| 11 | Turning | 16 | 15-25 | 24 | 26.4 |
| 12 | Turning | 32 | 15-25 | 21 | 23.1 |
| 13 | Turning | 64 | | 60 | 66 |
| 14 | Turning | 128 | 115-140 | 90 | 99 |
| 15 | Lapping | 4 | | 7.5 | 8.25 |
| 16 | As Rec'd | - | | 24 | 26.4 |

## TABLE III

## STAINLESS STEEL 17-7PH

### Surface Roughness

| Specimen | Surface Preparation | Nominal Roughness | Measured Roughness | | |
|---|---|---|---|---|---|
| | | | Profilometer rms | Tally CLA | Surf rms |
| S-1 | CGHP | ≈45 | 95-110 | 90 | 99 |
| 2 | FGHP | ≈48 | 50-65 | 60 | 66 |
| 3 | Grinding | 16 | | 42-52 | 46.2-57.2 |
| 4 | Grinding | 32 | | 28-36 | 30.8-39.6 |
| 5 | Grinding | 64 | | 16 | 17.6 |
| 6 | Milling | 16 | | | |
| 7 | Sand Paper | 16 | | 10-22 | 11-24.2 |
| 8 | Sand Paper | 32 | | | |
| 9 | Milling | 32 | | 35 | 38.5 |
| 10 | Milling | 64 | | | |
| 11 | Turning | 16 | | 32 | 35.2 |
| 12 | Turning | 32 | | 30 | 33 |
| 13 | Turning | 64 | | 30 | 33 |
| 14 | Turning | 128 | | 70 | 77 |
| 15 | Lapping | 4 | | | |
| 16 | As Rec'd | - | | 55-70 | 60.5-77 |

S-1, S-2 were the only specimens not annealed at Avco.

$$V_{ss} = \left(\frac{\pi}{3}\right)(h^2)\ (3r-h) \qquad (2)$$

where: $V_{ss}$ = volume of a spherical segment, $in^3$

h = height of the segment from base plane, in.

r = radius of the sphere, in.

x = radius of the segment at the base plane, in.

By combining the two equations and solving for r:

$$r = \left(\tfrac{1}{2}\right)\left(h + \frac{x^2}{h}\right) \qquad (3)$$

Using the contact angle cosine relationship:

$$\cos\theta = \frac{(r - h)}{r} \qquad (4)$$

equation (3) is substituted for r:

$$\cos\theta = \frac{x^2 - h^2}{x^2 + h^2} \qquad (5)$$

By simply measuring the liquid droplet diameter (2X) and its height (h) using any of the various metrology techniques, a suitably accurate value for cos θ can be easily obtained. An even greater simplification is made by taking the ratio of droplet height and diameter (h/2x), which normalizes equation (5) for any case (not too large a droplet). This ratio versus contact angle cosine is presented in Figure 4. For comparison, this ratio is plotted versus contact angle (θ) in Figure 5.

2. Light reflection technique development

The as-prepared substrate plates were nondestructively evaluated at selected points using two different light reflection techniques. The main object of this work was to compare values from both techniques, looking for consistency with prior work and consistency between techniques. The Photovolt Photoelectric Glossmeter, Model 610/Search Unit Type 660-M (Figure 6) served as the basis for one technique. A Watkins-Johnson Helium-Neon Laser, Type WJ-291/EG&G Lite-Mike, Model 560/Hewlett Packard DC Null Voltmeter, Type 419A/BB&N Plotamatic X-Y Recorder, Model 800-A (Figure 7) served as the basis for the other technique. White light and red light 45° reflection results, both on a 0-100 arbitrary scale, are given in Table IV. These results did show, in fact, that identical or very similar reflection energy values were obtained from both techniques, and with similar ranking.

The whole reason for using 6" x 6" plates rather than classical adhesive bond specimens was to provide a reasonably large area that could be expected

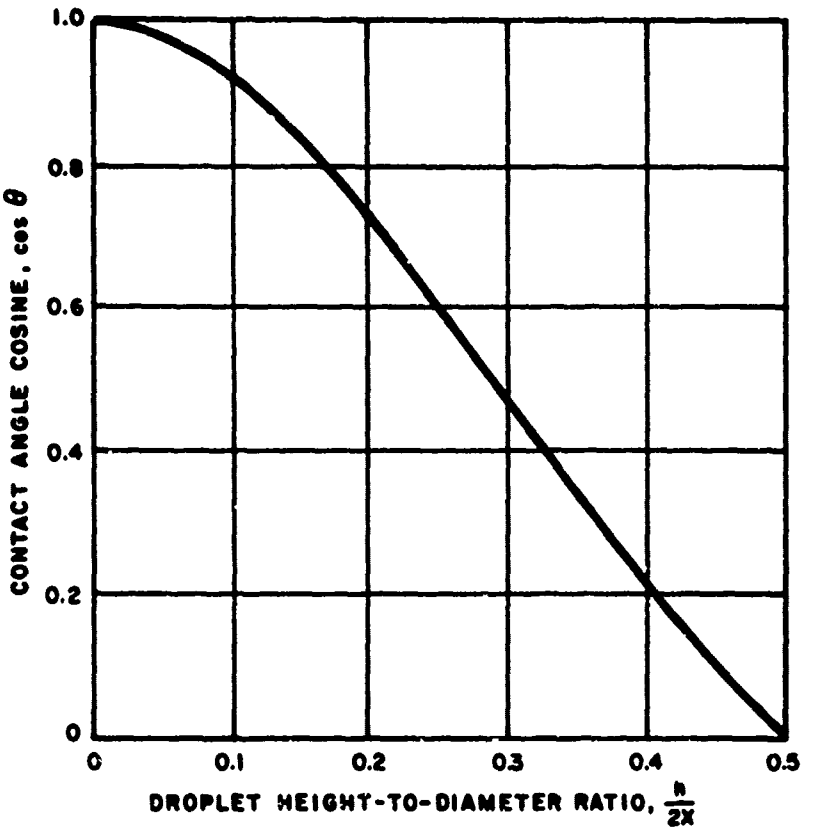


Figure 4 CALCULATION OF ANGLE COSINE AS FUNCTION OF NORMALIZED LIQUID DROPLET HEIGHT.

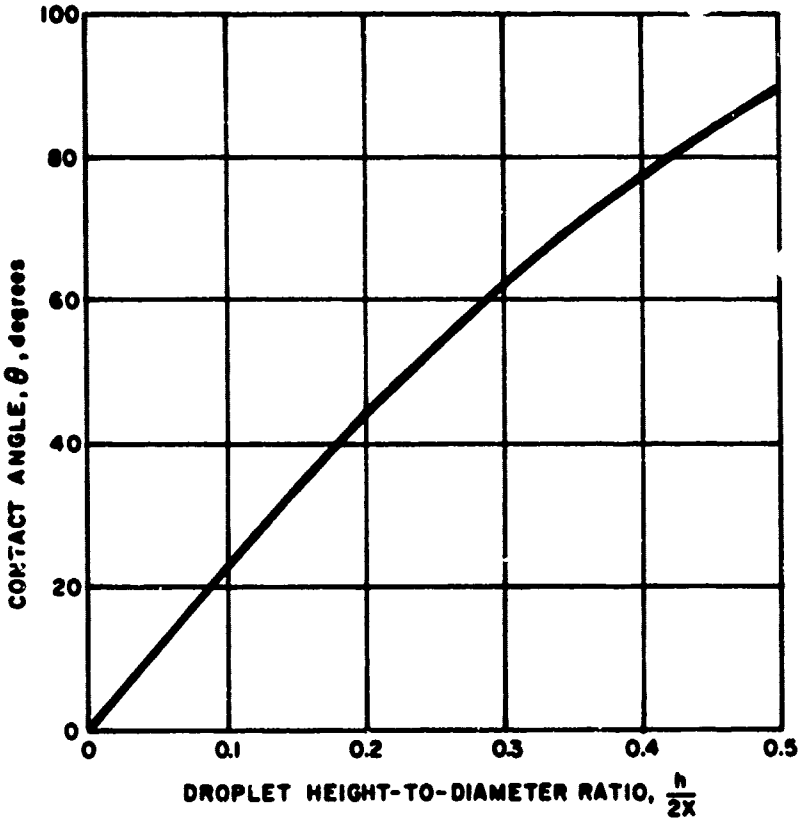


Figure 5 CALCULATION OF CONTACT ANGLE AS A FUNCTION OF NORMALIZED LIQUID DROPLET HEIGHT.

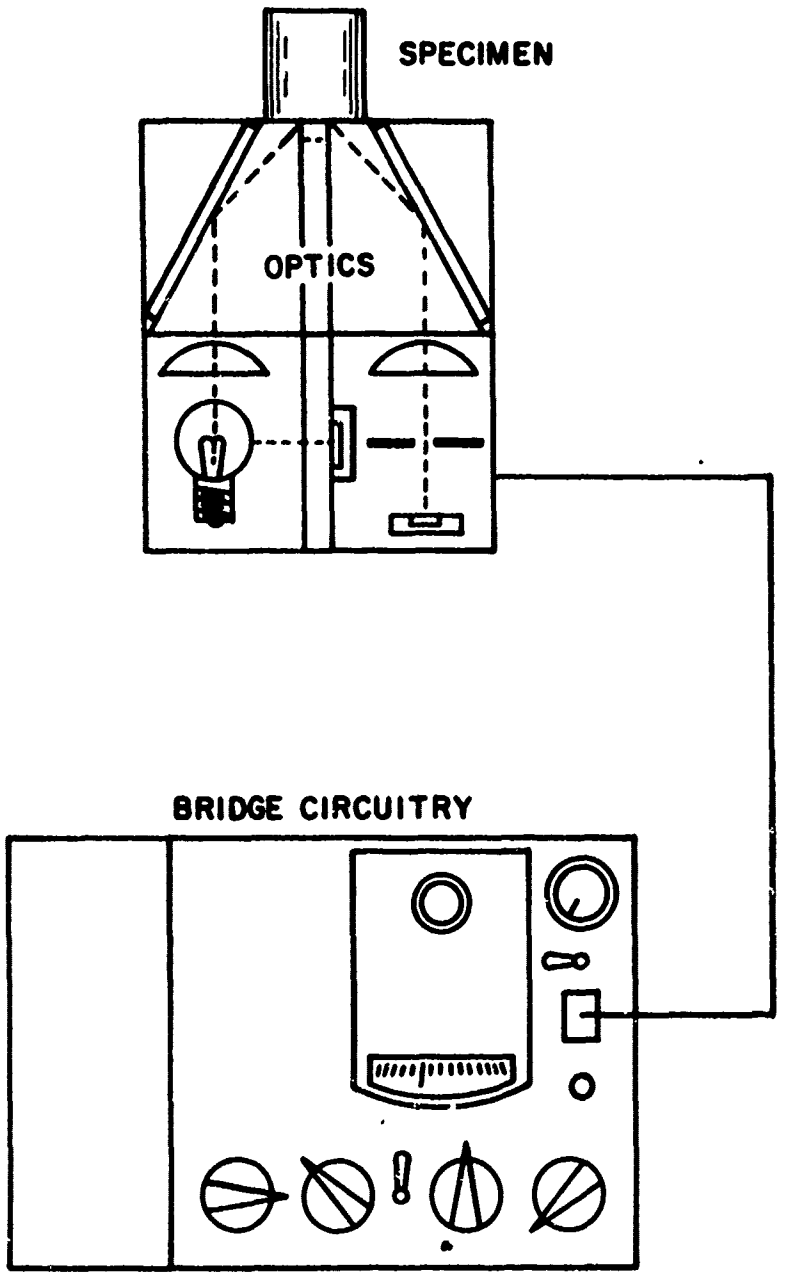


FIGURE 6. LIGHT REFLECTION TECHNIQUE USING A PHOTOVOLT GLOSSMETER.

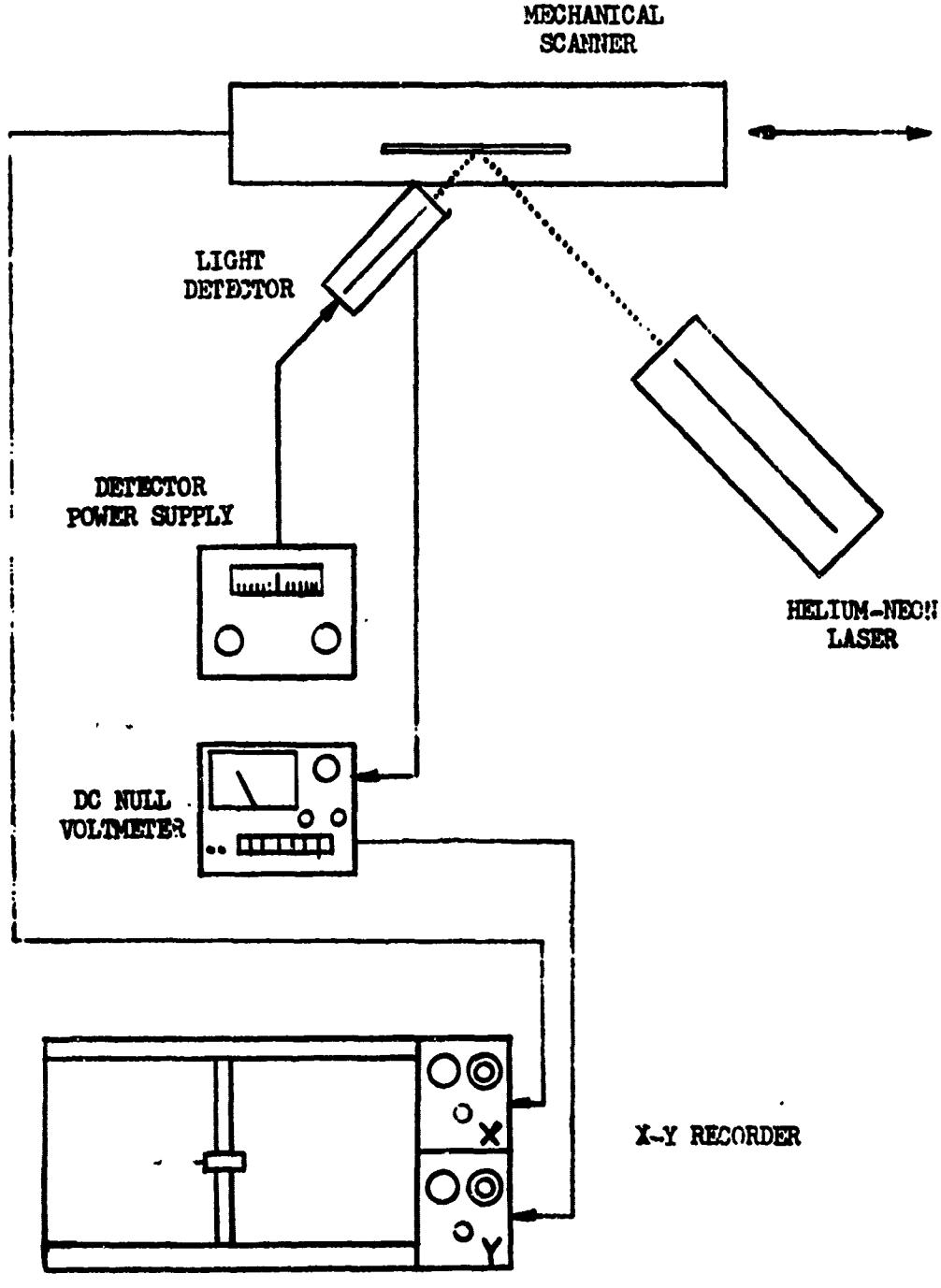


FIGURE 7. LIGHT REFLECTION TECHNIQUE USING A HELIUM-NEON LASER SOURCE AND SEPARATE LIGHT ENERGY DETECTOR.

## TABLE IV

### Comparison of Light Reflection Techniques

| ALUMINUM | | | TITANIUM | | | STAINLESS STEEL | | |
|---|---|---|---|---|---|---|---|---|
| Specimen No. | Relative Reflection | | Specimen No. | Relative Reflection | | Specimen No. | Relative Reflection | |
| | Laser | Glossmeter | | Laser | Glossmeter | | Laser | Glossmeter |
| A-1 | 5 | 1 | T-1 | 2 | $1^{H}$ - $1^{V}$ | S-1 | 3 | $1^{H}$ - $1^{V}$ |
| 2 | 4 | 0.4 | 2 | 2 | $1^{H}$ - $1^{V}$ | 2 | 3 | $1^{H}$ - $1^{V}$ |
| 3 | $100^{H}$-$43^{V}$ | $100^{H}$-$40^{V}$ | 3 | $20^{H}$-$7^{V}$ (V. Ripple) | $17^{H}$-$7^{V}$ | 3 | $22^{H}$-$15^{V}$ | $18^{R}$-$7^{V}$ |
| 4 | $37^{H}_{D}$-$43^{S}$ | $28^{D}$-$40^{S}$ | 4 | $16^{H}$-$10^{V}$ | $17^{H}$-$8^{V}$ | 4 | $18^{S}$ - 9 | 10 |
| 5 | $27^{S}$-$21^{D}$ | $11^{D}$-$16^{S}$ | 5 | $17^{H}$-$8^{V}$ | $14^{H}$-$6^{V}$ | 5 | $31^{H}$-$10^{V}$ | $30^{H}$-$13^{V}$ |
| 6 | $80^{H}$-$40^{V}$ | $57^{H}$-$22^{V}$ | 6 | $6^{H}$ - $2^{V}$ | $2^{H}$ - $1^{V}$ | 6 | 3 | $1^{H}$ - $1^{V}$ |
| 7 | 54 | 46 | 7 | upright 13 | $32^{H}$-$25^{V}$ | 7 | $53^{H}$-$51^{V}$ | $38^{H}$-$38^{V}$ |
| 8 | $29^{H}$-$21^{V}$ | $21^{H}$-$10^{V}$ | 8 | $37^{H}$-$26^{V}$ | $27^{H}$-$15^{V}$ | 8 | $17^{H}$-$13^{V}$ | $13^{H}$-$9^{V}$ |
| 9 | $42^{H}$-$100^{V}$ | $66^{H}$-$15^{V}$ | 9 | $50^{H}$-$28^{V}$ | $60^{H}$-$24^{V}$ | 9 | V grain 25 | $35^{H}$-$16^{V}$ |
| 10 | $38^{H}$-$25^{V}$ | $72^{H}$-$16^{V}$ | 10 | | | 10 | 4 | $1^{H}$ - $1^{V}$ |
| 11 | $61^{C}$-$36^{R}$-$38^{L}$ | $65^{C}$-$33^{R}$-$27^{L}$ | 11 | $42^{C}$-$35^{R}$-$33^{L}$ | $49^{C}$-$28^{R}$-$24^{L}$ | 11 | $36^{C}$-$26^{R}$-$30^{L}$ | $33^{C}$-$17^{R}$-$21^{L}$ |
| 12 | $81^{C}$-$43^{R}$-$43^{L}$ | $87^{C}$-$35^{R}$-$42^{L}$ | 12 | $64^{C}$-$44^{R}$-$48^{L}$ | $58^{C}$-$32^{R}$-$35^{L}$ | 12 | $13^{C}$-$37^{R}$-$28^{L}$ | $12^{C}$-$28^{R}$-$28^{L}$ |
| 13 | $77^{C}$-$42^{R}$-$48^{L}$ | $83^{C}$-$29^{R}$-$36^{L}$ | 13 | $59^{C}$-$54^{R}$-$60^{L}$ | $64^{C}$-$23^{R}$-$25^{L}$ | 13 | $30^{C}$-$17^{R}$-$18^{L}$ | $41^{C}$-$12^{R}$-$12^{L}$ |
| 14 | $74^{C}$-$35^{R}$-$42^{L}$ | $79^{C}$-$39^{R}$-$45^{L}$ | 14 | $50^{C}$-$43^{R}$-$35^{L}$ | $57^{C}$-$21^{R}$-$24^{L}$ | 14 | $31^{C}$-$49^{R}$-$51^{L}$ | $37^{C}$-$24^{R}$-$30^{L}$ |
| 15 | 105 | 84-$94^{C}$ | 15 | 3 | $1^{H}$ - $1^{V}$ | 15 | 3 | $1^{H}$ - $1^{V}$ |
| 16 | 74 | $72^{H}$ - $42^{V}$ | 16 | upright 4 | $2^{H}$ - $2^{V}$ | 16 | 5 | $4^{H}$ - $4^{H}$ |
| | | | | | | S-2 Reverse Side | 8 | $4.5^{H}$-$4.5^{V}$ |

Superscript Code:
H = Horizontal Lay
V = Vertical Lay
L = Left Third
C = Center Third
R = Right Third
D = Apparent Dull Area
S = Apparent Shiny Area

to contain variability in surface free energy, contact angle and therefore bond adhesive strength, as well as be suitable for area scanning. The laser-based technique was used to provide horizontal line scans for red light reflection energy, with vertical indexing. Spectacular results (Figure 8) were obtained from Plate S-4 (Stainless Steel)(Figure 9) which had warped during surface grinding, using a 1/8" scan index. Figure 10, for Plate A-3 (Aluminum), using a $\frac{1}{4}$" scan index, shows a smeared area in one corner which occurred during surface grinding. The vertical line indication was due to a wet-finger streak intentionally applied after grinding. In Figure 11, Plate T-14 (Titanium), using a $\frac{1}{4}$" scan index, the circular pattern resulting from lathe turning can be observed as a "double-vee" (dashed lines). Here the familiar qualitative impression gained from visual inspection of a plate can be produced quantitatively through these measurements.

C. Specimen Surface Preparation and Evaluation

Following the white light and laser red light characterization of the as-machined surfaces, two 6" x 6" panels of each substrate material were cut into 2" x 2" squares. The previously machined surfaces were masked so they would not be further disturbed during cutting. The resulting 18 squares/2" x 2") were then submitted for additional adhesive bonding surface preparation and scheduled contamination. Individual specimen locations as cut from the 6" x 6" plates were identified typically as shown in the aluminum layout diagram of Figure 12. In this manner, individual 2" x 2" specimens could be referred to the white light and laser red light surveys of surface roughness previously recorded.

Aluminum studs, 3/4" diameter (6061-T6 alloy) were fabricated for use in preparing the adhesive bond specimen shown in Figure 13. The 54 studs were grit blasted and identified to correspond with the 54 2" x 2" x 1/8" squares. Stud lengths and 2" x 2" square thickness were measured at the center of each square for subsequent control of bond line thickness. All aluminum studs and squares, as well as the titanium and stainless steel squares were then cleaned using the procedures shown in Appendix I.

Following cleaning, all studs were primed by spraying with Bloomingdale, MMS 307, Type II, corrosion inhibited adhesive primer. The squares were deliberately contaminated in accordance with the schedule shown in Table V after which they were evaluated by infrared and ultraviolet spectrophotometric scans. The squares were then primed with the MMS 307, Type II primer (BR 400). Priming was applied in $\frac{1}{4}$ to $\frac{1}{2}$ mil thickness, air dried at room temperature for 30 minutes minimum, then oven cured at 200°F for 30 minutes.

1. Spectrophotometric evaluation

Evaluation of the deliberately contaminated 2" x 2" squares by spectrophotometric techniques was accomplished with the goal of finding absorption peaks which could be employed for quantitative characterization of significant bond strength limiting parameters. The apparatus used for these measurements was an extended-range Beckman DK-2 ratio recording spectrophotometer (Figure 14). The instrument characteristics are given in Table VI. The various experiments which can be performed with the instruments are summarized in Table VII. For the particular characterization

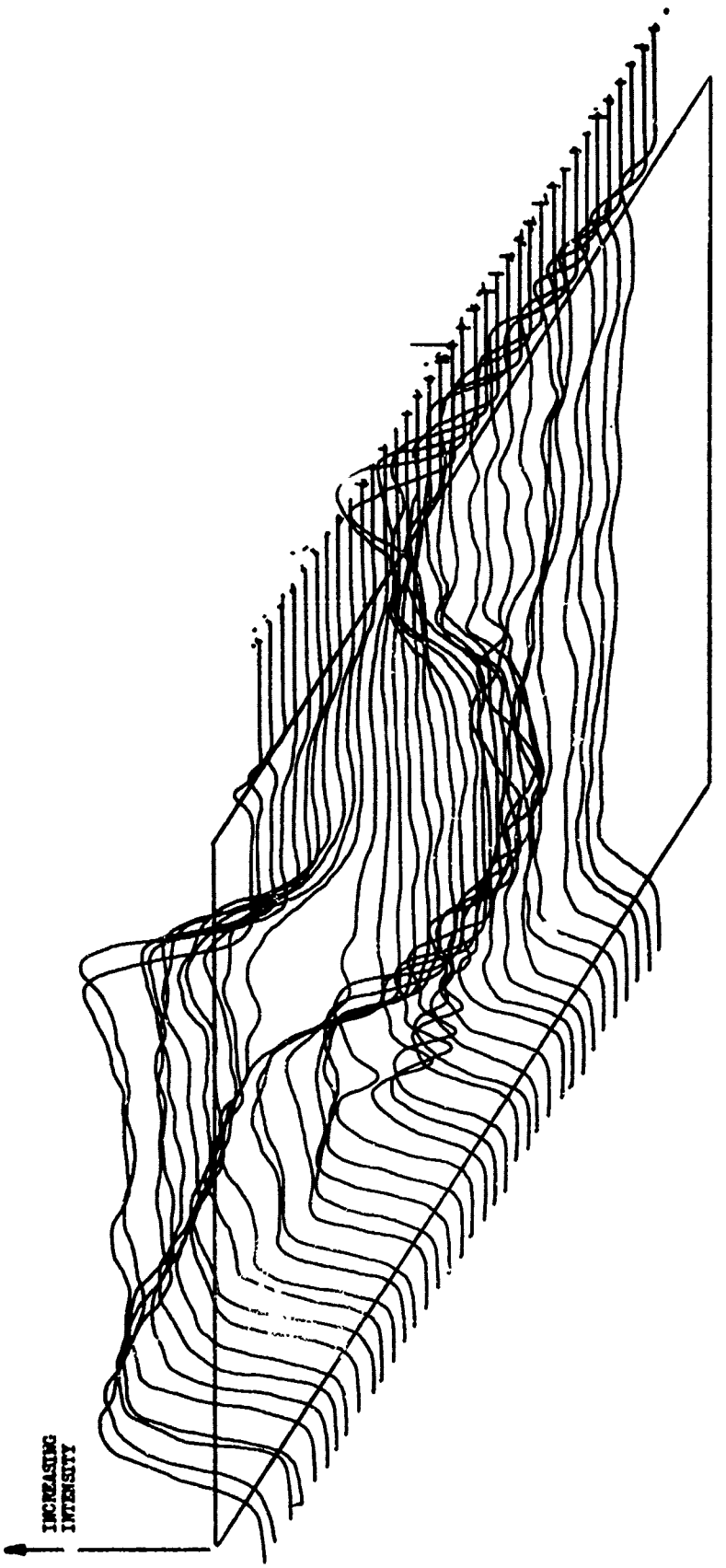


FIGURE 8. HORIZONTAL SCAN WITH 1/8" VERTICAL INDEX ON STAINLESS STEEL PLATE S-4 USING THE RED LASER LIGHT REFLECTION TECHNIQUE

FIGURE 9. PHOTOGRAPH OF PLATE S-4 FOR COMPARISON WITH SCAN INFORMATION (PURPOSELY INVERTED).

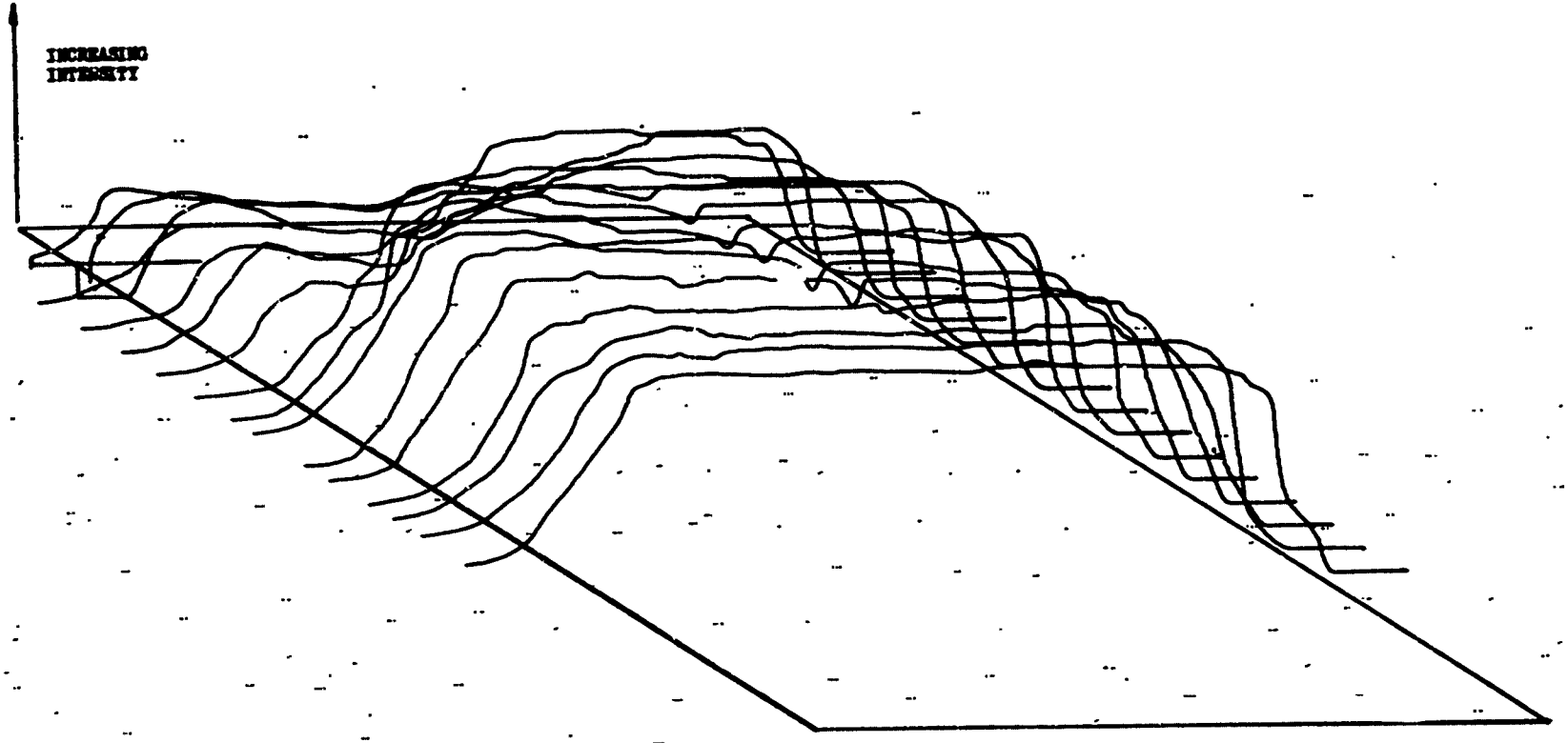


FIGURE 10. HORIZONTAL SCAN WITH $\frac{1}{4}$" VERTICAL INDEX ON ALUMINUM PLATE A-3 USING THE RED LASER REFLECTION TECHNIQUE.

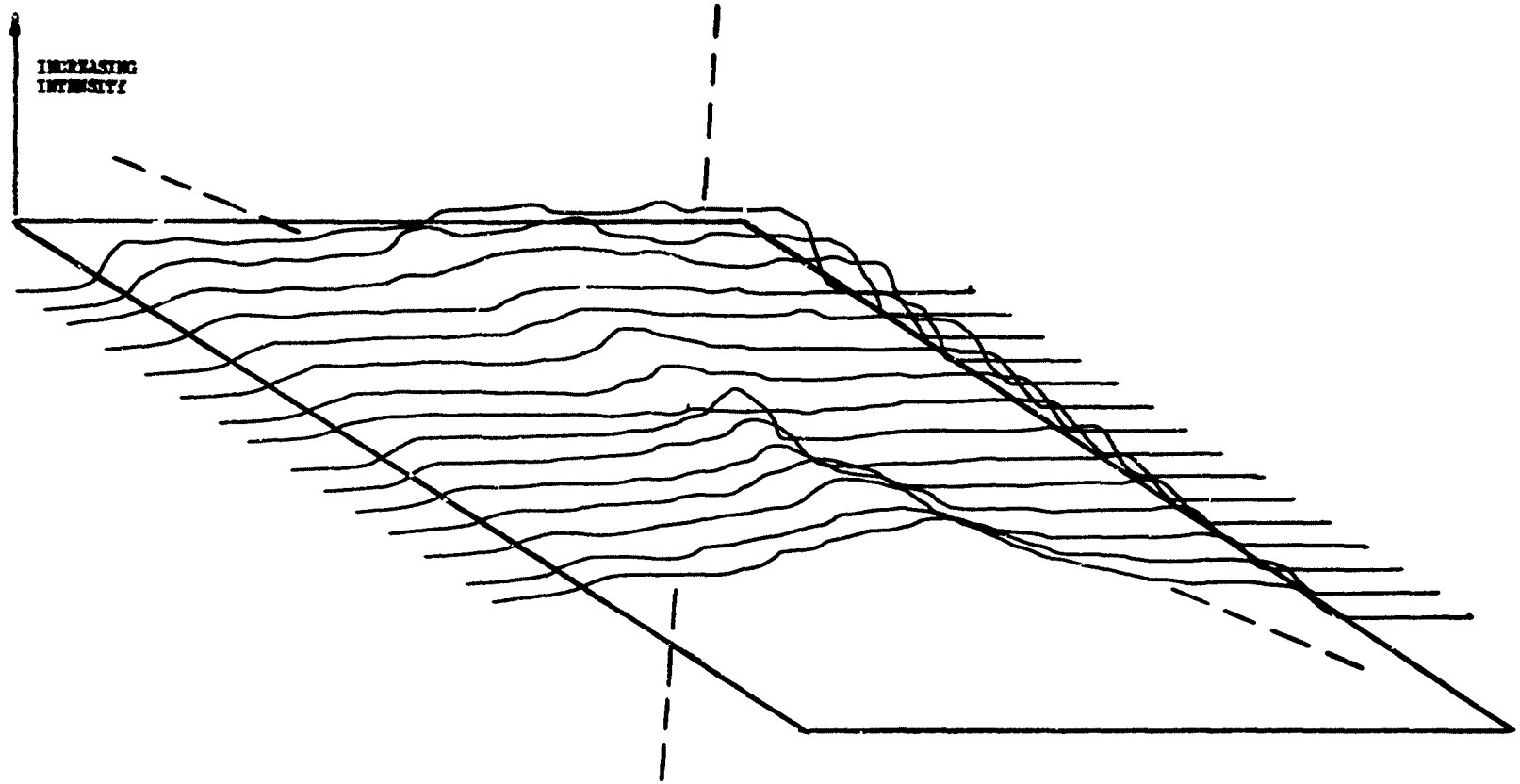


FIGURE 11. HORIZONTAL SCAN WITH $\frac{1}{4}$" VERTICAL INDEX ON TITANIUM PLATE T-14 (CIRCULAR LATHE-TURNED PATTERN).

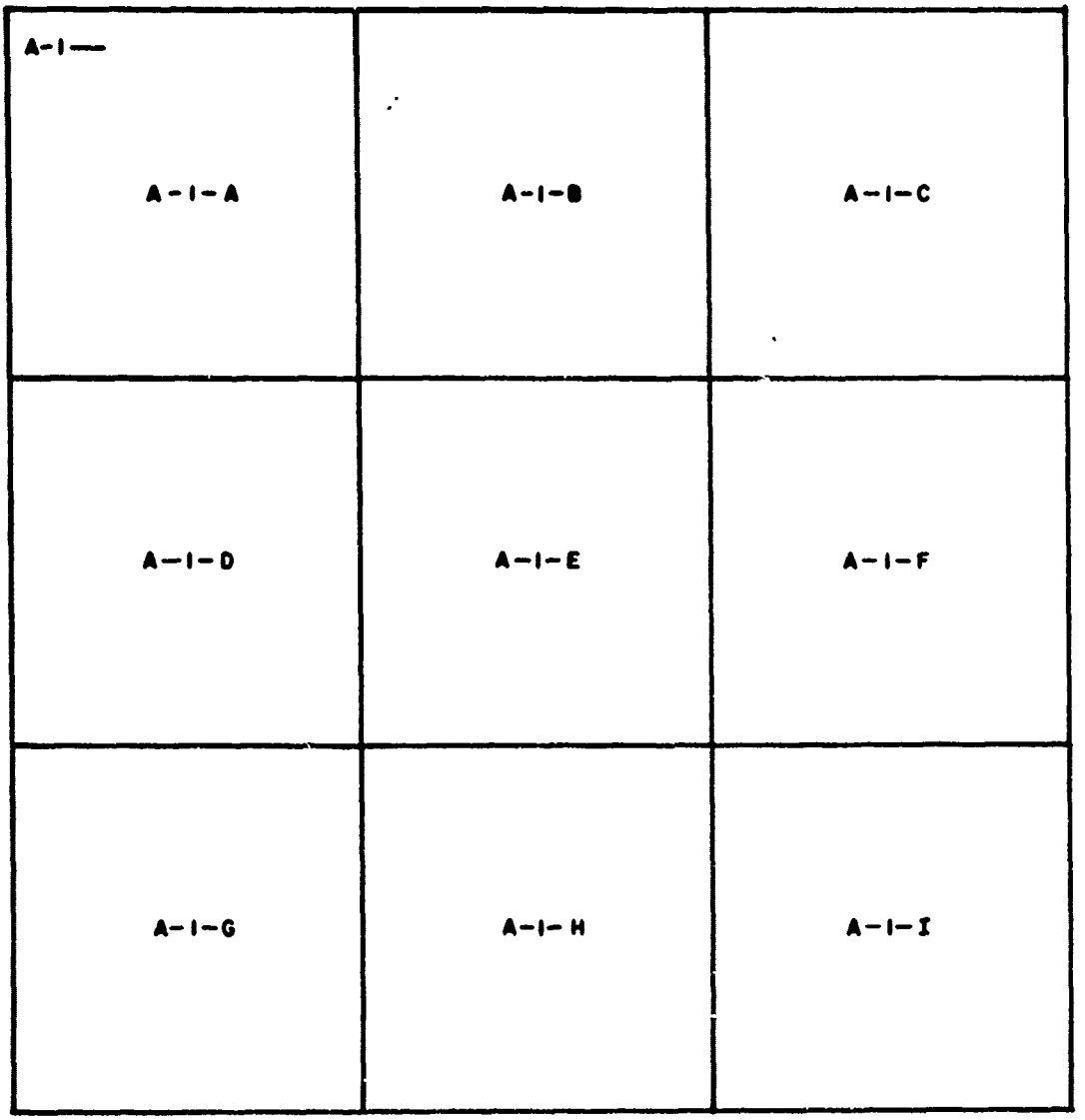


Figure 12 TYPICAL SPECIMEN LAYOUT FOR ALUMINUM 6" X 6" X 1/8" PLATE.

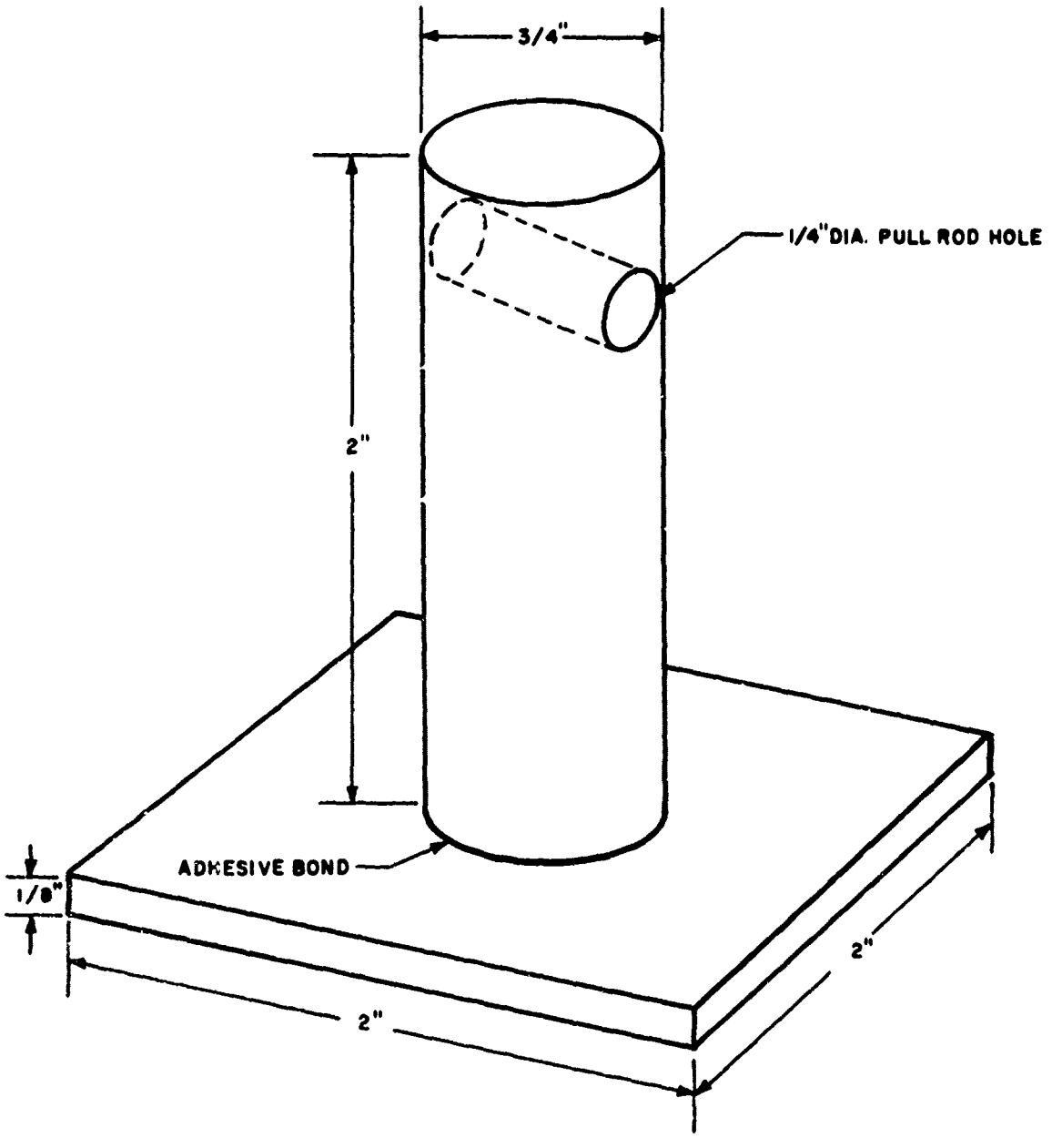


Figure 13 ADHESIVE BOND SPECIMEN.

## TABLE V

### Contamination Procedures

NOTE: All specimens are to be handled as if clean except for purposeful contamination.

A1A, A1B, A1C - Clean
T1A, T1B, T1C - Clean
S1A, S1B, S1C - Clean

A1D, A1E, A1F - Body sweat contamination (fingerprint)
T1D, T1E, T1F - Body sweat contamination (fingerprint)
S1D, S1E, S1F - Body sweat contamination (fingerprint)

A1G, A1H, A1I - floor dust
T1G, T1H, T1I - floor dust
S1G, S1H, S1I - floor dust
} wipe off with dry cloth or blow off with compressed air

A2A, A2B, A2C
T2A, T2B, T2C
S2A, T2B, T2C
} Run on spectrophotometer before and after contamination

{ Overage - 150°F, 50% RH, 4 hrs.
{ Overage - 150°F, 50% RH, 4 hrs.
{ Overage - 150°F, 50% RH, 4 hrs.

A2D, A2E, A2F - Incomplete rinse after surface preparation
T2D, T2E, T2F - Incomplete rinse after surface preparation
S2D, S2E, S2F - Incomplete rinse after surface preparation

A2G, A2H, A2I - Mold release overspray
T2G, T2H, T2I - Mold release overspray
S2G, S2H, S2I - Mold release overspray
} Set specimens near a dummy plate and spray dummy plate. Do not spray specimens directly.


Figure 14 BECKMAN DK-2 RATIO RECORDING SPECTROPHOTOMETER

## TABLE VI

### Beckman Recording Spectrophotometer Specifications

| | |
|---|---|
| Wavelength Range | 185 to 3500 mμ |
| Wavelength Calibration Accuracy | |
| Ultraviolet | ± 0.4 mμ |
| Visible | ± 1.5 mμ |
| Near-Infrared (110 to 2000) | + 10 to -15 mμ |
| 200 to 3500 | ± 8 mμ |
| Transmittance Ranges (percent) | 0-100, 0-10, 75-125, 90-100, 90-110, 95-105, and 0-200 |
| Absorbance Ranges | 0-1, 0.5-1.5, and 0.2 to 0.7 |
| Chart Speeds (inches/min) | 0.5, 1, 1.5, 3, 5, 10, or 15 |
| Scanning Speeds (min. to cover 4/5 of wavelength scroll rev.) | 1, 3, 10, 30, or 100 |

### Source and Detector Ranges

| Wavelength Range, mμ | Source | Detector |
|---|---|---|
| 550-2700 | W | PbS |
| 320-750 | W | P.M.* |
| 210-370 | $H_2$ | P.M. |

*Photomultiplier

## TABLE VII

### Summarizing Modes of Operation

| Mode of Operation | Type of Determination: Reflectance (see Figure C-5) — Diffuse | Reflectance (see Figure C-5) — Total | Transmittance (see Figure C-4) — Diffuse | Transmittance (see Figure C-4) — Total | Fluorescent |
|---|---|---|---|---|---|
| Monochromatic Illumination | Mgo in reference exit port & sample in sample exit port.<br><br>Sample & reference normal to entrance beam.<br><br>Sample & reference must have same specular characteristics.<br><br>Incorrect result when sample fluorescent. | MgO in reference exit port & sample in sample exit port.<br><br>Sample & reference placed at 5-degree angle to entrance beam.<br><br>Variation in surface textures of sample & reference not as critical as for diffuse reflectance.<br><br>Incorrect results when sample fluorescent. | MgO in reference exit port. Sample exit port open.<br><br>Diffuse sample in entrance sample port.<br><br>Reference entrance open.<br><br>Incorrect results when sample fluorescent. | MgO in sample & reference exit ports.<br><br>Excellent technique for samples which are highly diffusive or which diffuse nonuniformly.<br><br>Incorrect results when sample fluorescent. | MgO in reference exit port & sample in sample exit port.<br><br>Useful for determining spectral distribution of energy producing fluorescence.<br><br>Use appropriate filter in front of detector to eliminate effect of energizing spectra; this permits only fluorescent light to reach detector. |
| Monochromatic Detection | Sample & reference in exit ports.<br>Specular shift plates in DIFFUSE position.<br>Gives correct reflectance for fluorescent samples.<br>Spectral intensity of source must be controlled if sample is fluorescent. | | Sample & reference in entrance ports.<br>MgO in both exit ports.<br>Gives correct reflectance for fluorescent samples.<br>Spectral intensity of source must be controlled if sample is fluorescent. | | Use appropriate filter to eliminate fluorescent light & permit only fluorescence-energizing wavelengths to enter sphere. |
| Spectro-radiometry | All ports open.<br><br>Sample and reference sources mounted externally. | | | Detector mounted in same position as for monochromatic detection. | |

study conducted in this work, the total reflectance measurement depicted diagrammatically in Figures 15 and 16 was employed so that both the specular and diffuse components of reflectance are integrated into the sphere. All spectral measurements were made with reference to magnesium oxide taken as approximately 100%. A 0% reflectance level can be established on the chart by interrupting the light beam normally falling on the MgO reference specimen. The 2" x 2" squares then provide traces representing their total reflectance relative to these 100% and 0% reference levels over the range of 0.5 to 2.7 microns (near IR) and 0.225 to 0.7 microns (UV). These ranges involve considerable overlap into the visible spectrum in addition to the IR and UV regions.

A chart showing the reference levels and gross examples of contamination is shown in Figure 17. Starting from the bottom of the chart, the 0% reference level is followed by the spectral reflectance in the IR region for a glass sample soiled with mystery oil mixed with dirt and just above it, a clean glass sample. No absorption peaks are seen in either of these scans. At mid-chart is shown an aluminum sample with a heavy coating of silicone grease, an aluminum sample with a heavy coating of silicone mold release agent, and an aluminum sample coated with a wiped-off layer of silicone grease. For these three scans, an absorption peak is evident near the 2.3 micron wavelength.

Expecting to see response to and quantitative discrimination between the various contaminants deliberately applied to the 2" x 2" plates, to be subsequently employed in the bond specimens, a complete set of 18 IR scans was made on the aluminum plates. Figure 18 shows the IR scan on clean aluminum. Figures 19 and 20 show IR scans for aluminum contaminated with a fingerprint (body sweat) and with floor dust, respectively. No significant difference could be detected between the clean and contaminated aluminum at the maximum available sensitivity.

Similar scans were made in the IR range and in the UV range with no significant response observed for any of the contaminants on any of the sample materials; aluminum, titanium, and stainless steel.

D. Adhesive Bonding

The evaluation of the 2" x 2" squares by spectrophotometric techniques was conducted expeditiously to minimize inadvertant contamination. About nine specimens were evaluated per day and then moved immediately to the bonding laboratory.

Bloomingdale, MMS 307, Type I, supported film adhesive (FM 400) was applied to the primed aluminum studs and then assembled to the central portion of the primed 2" x 2" square sheet material. Nine specimens were cured at one time on a 6" x 6", electrically heated, hydraulic press platen. 85 PSI pressure was employed during cure. The cure consisted of increasing the temperature from 75°F to 340°F minimum in approximately 50 minutes while maintaining 85 PSI pressure. Temperature was then held between 340°F and 360°F for one hour after which specimens were cooled under pressure to 150°F before removing from the press.

E. Evaluation of Bonded Specimens

Following adhesive bonding the overall dimensions of all specimens were

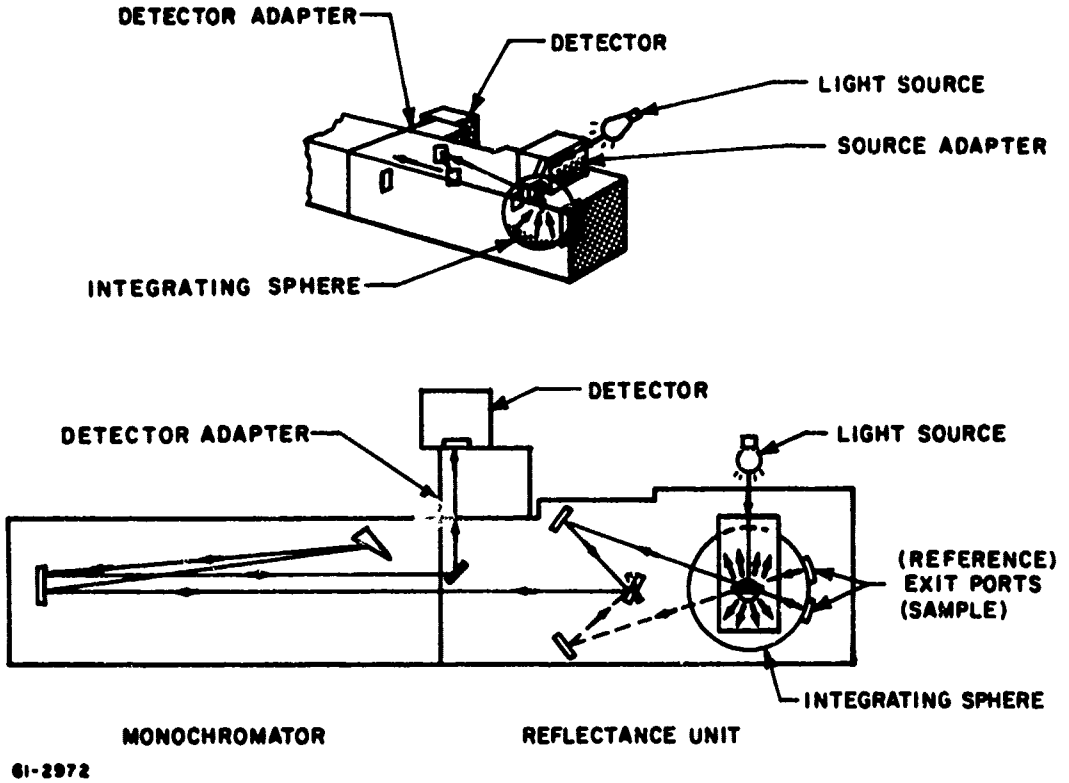


Figure 15 MONOCHROMATIC DETECTION LIGHT PATH.

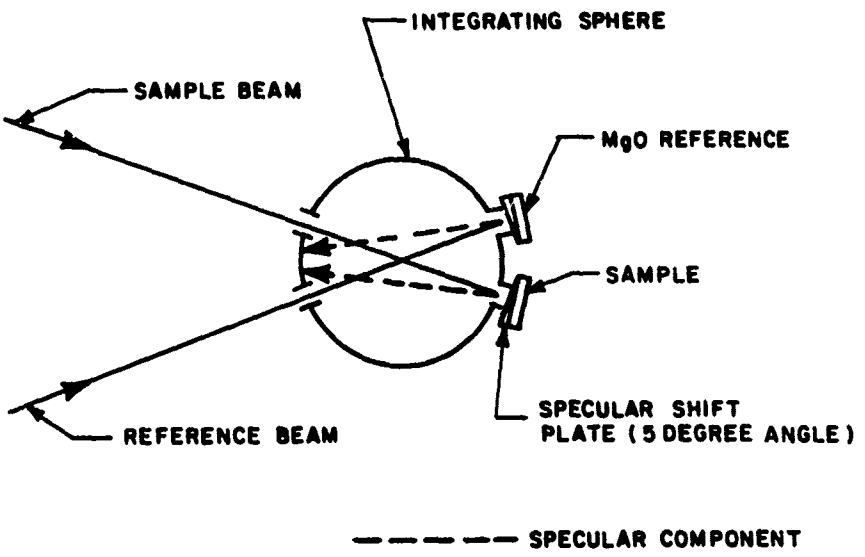


Figure 16 TOTAL REFLECTANCE ARRANGEMENT IN SPHERE.

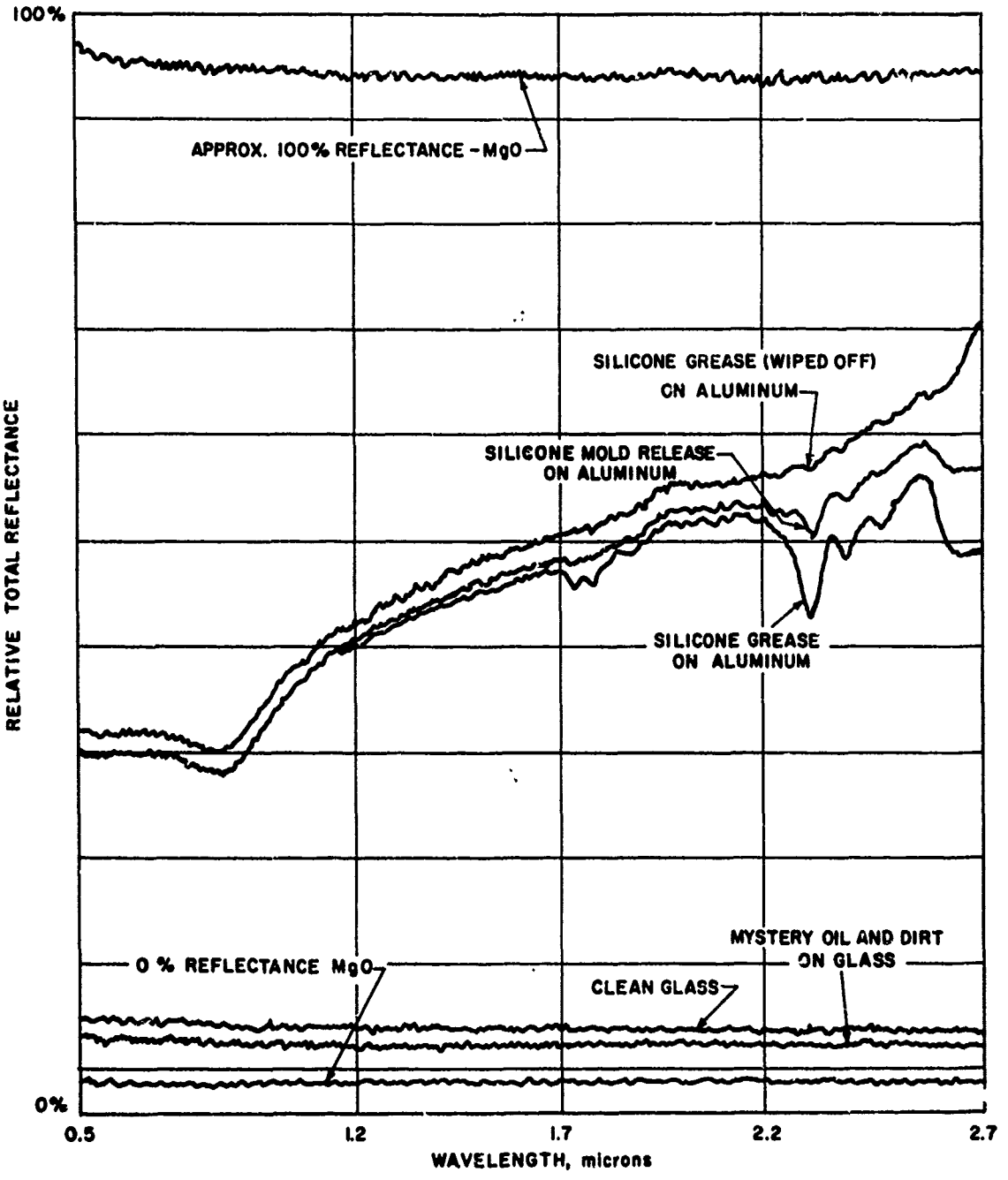


Figure 17 IR TOTAL REFLECTANCE FOR VARIOUS CONTAMINANTS.

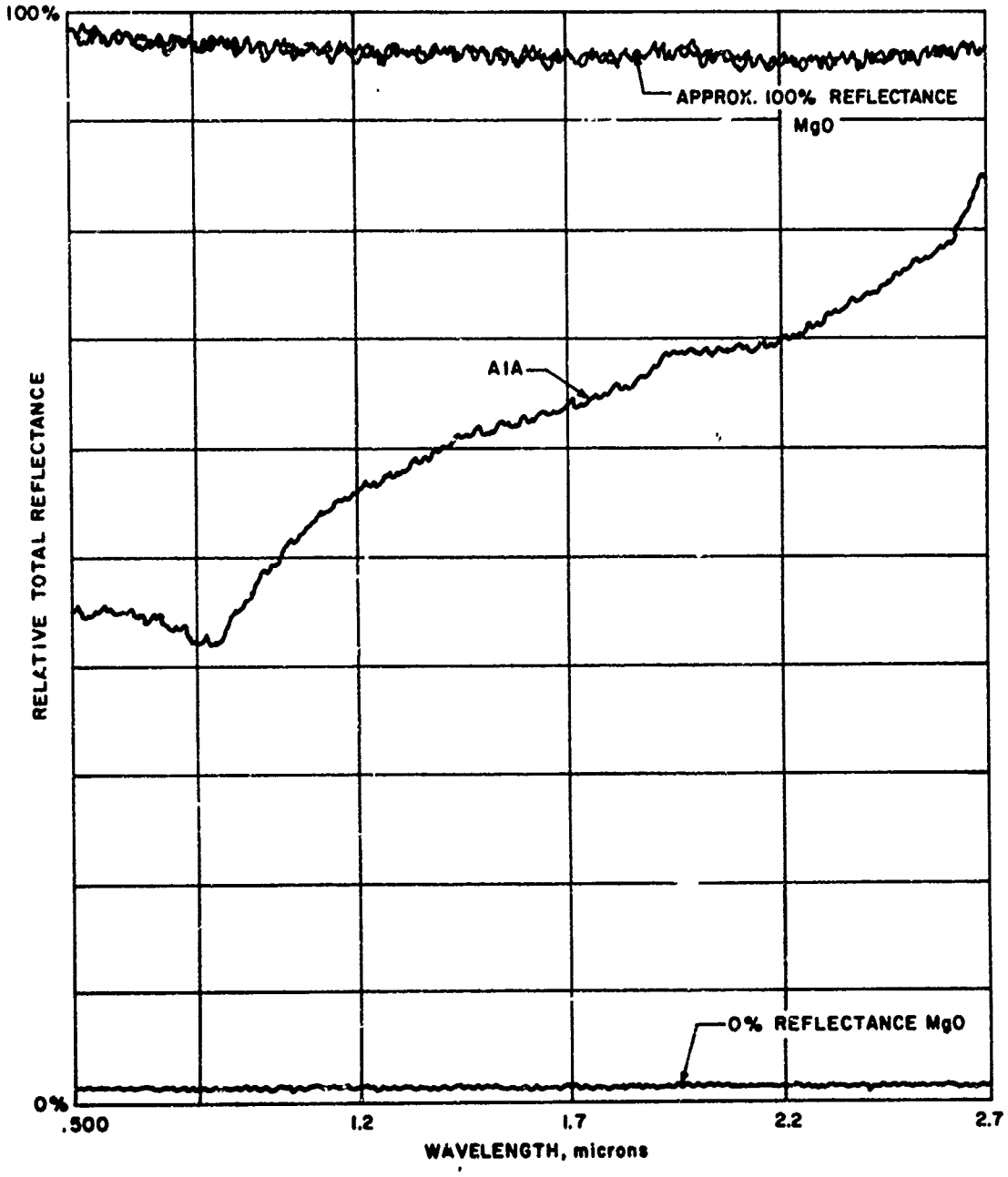


Figure 18 IR TOTAL REFLECTANCE SPECIMEN A1A-CLEAN ALUMINUM.

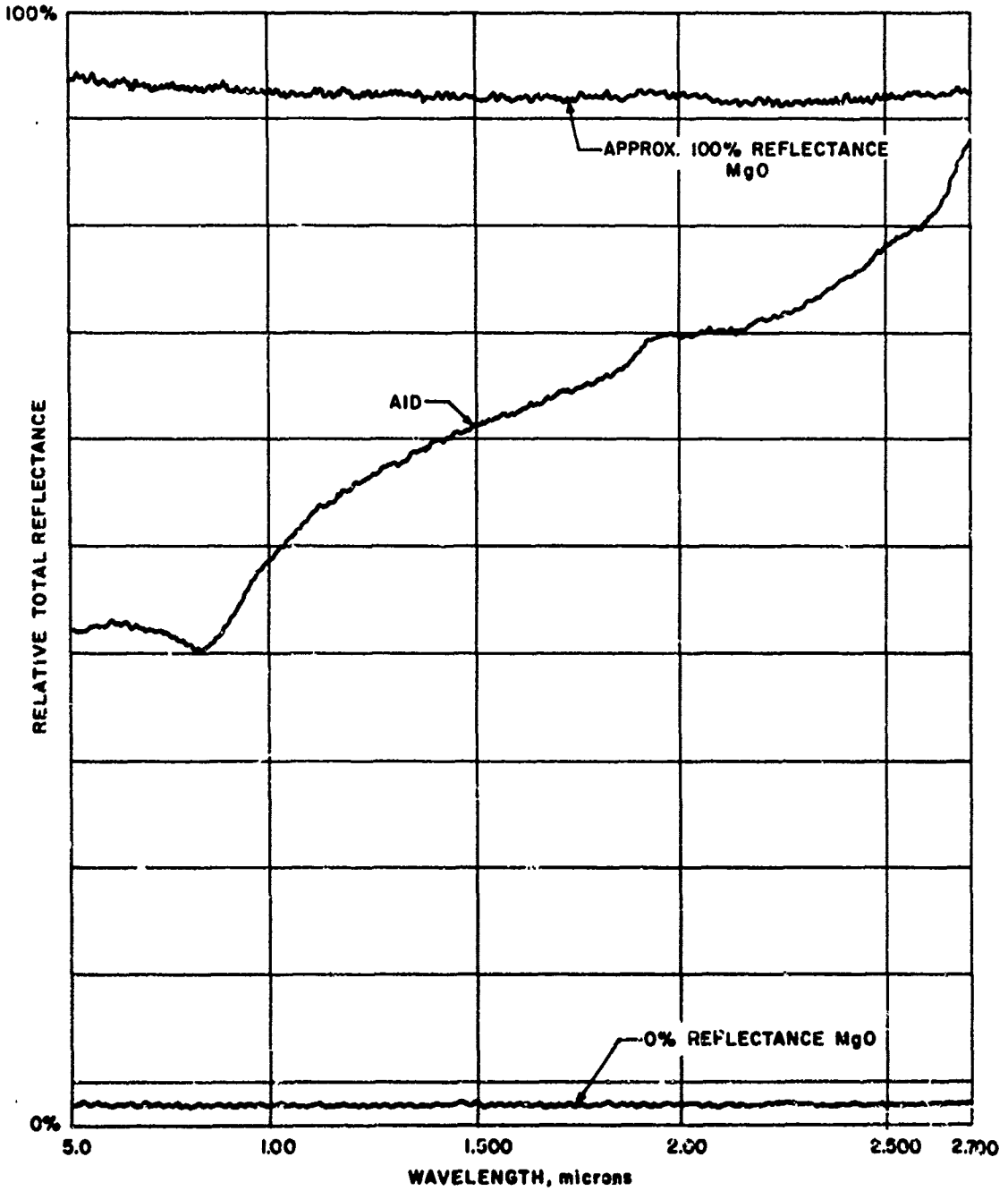


Figure 10 IR TOTAL REFLECTANCE SPECIMEN AID-FINGER PRINT ON ALUMINUM.

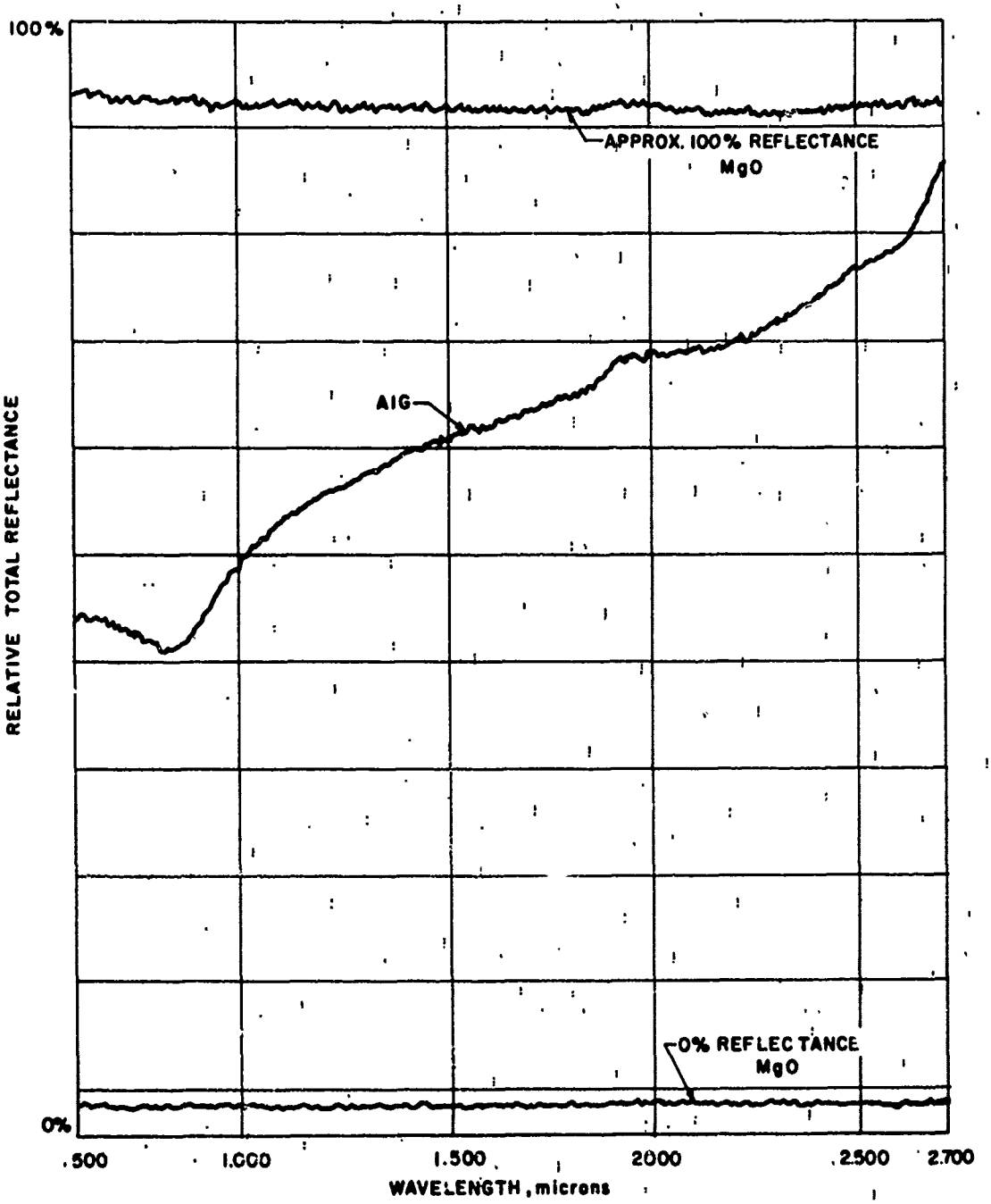


Figure 20 IR TOTAL REFLECTANCE SPECIMEN A1G-FLOOR DUST ON ALUMINUM.

measured (stud length plus bond line thickness plus 2" x 2" square thickness). By subtracting the sum of original square thickness and stud length, the bond line thickness was calculated and is shown in Table VIII.

All specimens were checked for perpendicularity between 2" x 2" square and pull-stud axis. This was a qualitative assessment using a simple right angle and visual inspection. One steel specimen, S1C, was found to have a warped 2" x 2" substrate and was dropped out of the subsequent tensile testing effort. Three titanium specimens, T2G-H and I, unbonded (fell apart) during the casual handling involved in checking perpendicularity. These specimens had been subjected to contamination with severe mold release overspray and were listed as having zero psi tensile strength.

Ultrasonic assessment of all remaining bonded specimens was accomplished using a Branson Sonoray instrument. Pulse-echo technique at 10 MHz frequency, 0.312 diameter Type SFZ (Automation Industries) transducer and water coupling, revealed apparently uniform, complete bonding for all specimens except those eliminated as discussed above.

F. Tensile Testing

Results of bond tensile tests are shown in Table IX. All tests were conducted at room temperature. Diameters and areas of bond joints were 0.750 inches and 0.442 square inches, respectively. Stress rate was 600/700 psi per minute.

In reviewing the types of fractures observed, the deliberate contaminants were successful in producing cohesive, adhesive, and mixed types. It can be assumed that the lowest strengths involving mixed fracture (partly adhesive, partly cohesive) are related to the amount of bond area involved in the adhesive type of fracture. Visual observation of fractured surfaces supported this assumption. The totally cohesive failures were the strongest, the totally adhesive failures were very weak or zero strength.

Considerable scatter in strength is seen for specimens given the same intended surface treatment. This is not regarded as unusual but adds considerable confusion to attempts to see clear trends of data. The overage treatment (A2A, B, C; S2A, B, C; T2A, B, C) seemed to yield a slight increase in strength for the aluminum and titanium but considerable increase for steel. This was a somewhat unexpected result. None of the contaminants provided real degradation leading to adhesive or mixed fractures in aluminum. Only the incomplete rinse (S2D, E, F) and mold release overspray (S2G, H, I) seemed to be effective in producing mixed or adhesive fractures in the steel specimens. All but two titanium specimens, including the "clean" control specimens (T1A, B, C) showed mixed or adhesive failures. This observation might be due to a lower effectiveness, generally, of the surface preparation used on the titanium specimens.

G. Correlations

Although the deliberate contaminants applied were successful in yielding a range of strengths and fracture types, the correlation of these with NDT results prior to bonding is not possible. The ultraviolet and infrared spectrophotometry was not sufficiently sensitive to detect any except the most severe applications of silicone grease or mold release.

## TABLE VIII

### Thickness - Bonded Specimens

| Plate No. | Total Thick. (in.) | Corrected* Plate + Stud Thickness (in) | Bondline Thickness (in.) | Plate No. | Total Thick. (ins.) | Corrected* Plate + Stud Thickness (in) | Bondline Thickness (ins.) | Remarks |
|---|---|---|---|---|---|---|---|---|
| A-1-A | 2.1300 | 2.1257 | 0.0043 | T-2-A | 2.1020 | 2.0970 | 0.0050 | |
| B | 2.1320 | 2.1266 | .0054 | B | 2.1180 | 2.1119 | .0061 | |
| C | 2.1285 | 2.1232 | .0053 | C | 2.1160 | 2.1110 | .0050 | |
| D | 2.1310 | 2.1265 | .0045 | D | 2.1220 | 2.1172 | .0048 | |
| E | 2.1325 | 2.1260 | .0065 | E | 2.1225 | 2.1155 | .0070 | |
| F | 2.1310 | 2.1247 | .0063 | F | 2.1270 | 2.1204 | .0066 | |
| G | 2.1230 | 2.1182 | .0048 | G | 2.1270 | 2.1209 | .0061 | Complete Unbond |
| H | 2.1300 | 2.1259 | .0061 | H | 2.1240 | 2.1165 | .0075 | Complete Unbond |
| I | 2.1310 | 2.1267 | .0043 | I | 2.1280 | 2.1225 | .0055 | Complete Unbond |
| A-2-A | 2.1290 | 2.1242 | .0048 | S-1-A | 2.1380 | 2.1335 | .0045 | |
| B | 2.1310 | 2.1248 | .0062 | B | 2.1240 | 2.1177 | .0063 | |
| C | 2.1295 | 2.1250 | .0045 | C | | No Test | | Plate warped |
| D | 2.1300 | 2.1240 | .0060 | D | 2.1305 | 2.1245 | .0060 | |
| E | 2.1320 | 2.1250 | .0070 | E | 2.1400 | 2.1332 | .0068 | |
| F | 2.1300 | 2.1242 | .0058 | F | 2.1370 | 2.1329 | .0041 | |
| G | 2.1305 | 2.1261 | .0044 | G | 2.1355 | 2.1302 | .0053 | |
| H | 2.1320 | 2.1249 | .0071 | H | 2.1345 | 2.1282 | .0063 | |
| I | 2.1290 | 2.1242 | .0048 | I | 2.1360 | 2.1315 | .0045 | |
| T-1-A | 2.1260 | 2.1220 | .0040 | S-2-A | 2.1400 | 2.1347 | .0053 | |
| B | 2.1275 | 2.1218 | .0057 | B | 2.1420 | 2.1360 | .0060 | |
| C | 2.1270 | 2.1232 | .0038 | C | 2.1385 | 2.1340 | .0045 | |
| D | 2.1285 | 2.1237 | .0048 | D | 2.1420 | 2.1372 | .0048 | |
| E | 2.1290 | 2.1230 | .0060 | E | 2.1420 | 2.1341 | .0079 | |
| F | 2.1305 | 2.1257 | .0048 | F | 2.1410 | 2.1342 | .0068 | |
| G | 2.1280 | 2.1234 | .0046 | G | 2.1410 | 2.1358 | .0052 | |
| H | 2.1225 | 2.1160 | .0065 | H | 2.1420 | 2.1353 | .0067 | |
| I | 2.1195 | 2.1140 | .0055 | I | 2.1390 | 2.1343 | .0047 | |

*Corrected due to etch (.0005" for aluminum and stainless steel; 0.0015 for Ti)

## TABLE IX

### Tensile Bond Test Results

| Specimen[1] No. | | | | | | |
|---|---|---|---|---|---|---|
| | A1A | A1D | A1G | A2A | A2D | A2G |
| | A1B | A1E | A1H | A2B | A2E | A2H |
| | A1C | A1F | A1I | A2C | A2F | A2I |
| Breaking Stress, psi | 1920 | 1390 | 1560 | 2160 | 2400 | 1570 |
| | 2070 | 1980 | 1790 | 2310 | 2310 | 1600 |
| | 1480 | 1710 | 1620 | 1700 | 2290 | 1740 |
| Fracture[2] Type | C | C | C | C | C | C |
| | C | C | C | C | C | C |
| | C | C | C | C | C | C |
| Specimen No. | S1A | S1D | S1G | S2A | S2D | S2G |
| | S1B | S1E | S1H | S2B | S2E | S2H |
| | S1C | S1F | S1I | S2C | S2F | S2I |
| Breaking Stress, psi | 1410 | 2300 | 1650 | 1540 | 630 | 140 |
| | 2070 | 2530 | 2430 | 2830 | 1760 | 240 |
| | -[3] | 1590 | 2060 | 1810 | 140 | 210 |
| Fracture Type | C | C | C | C | M | A |
| | C | C | C | C | M | A |
| | C | C | C | C | A | A |
| Specimen No. | T1A | T1D | T1G | T2A | T2D | T2G |
| | T1B | T1E | T1H | T2B | T2E | T2H |
| | T1C | T1F | T1I | T2C | T2F | T2I |
| Breaking Stress, psi | 1130 | 1190 | 730 | 1300 | 1150 | 0[4] |
| | 1570 | 1560 | 1460 | 1600 | 1450 | 0 |
| | 1070 | 750 | 1270 | 1230 | 1810 | 0 |
| Fracture Type | M | M | M | C | M | A |
| | M | M | M | M | M | A |
| | M | M | M | M | C | A |

[1]Specimen No.: A-aluminum, S-stainless steel, T-titanium

[2]Fracture Type: C-cohesive, A-adhesive, M-mixed

[3]No test: substrate warped

[4]Severe overspray - release agent, fell apart in handling.

While white light and red laser reflectance measurements were found sensitive to various surface finishes as produced by machining techniques, surface roughness (CLA) was found to have little influence on bond strength during the previous year's work.[2]

## REFERENCES


1. Lockyer, G.E. and E.A. Proudfoot, "Development of Nondestructive Tests for the Evaluation of Bonded Materials," Technical Report No. AVATD-0123-69-CR (Avco) for Naval Air Engineering Center.

2. Zurbrick, J.R., "Nondestructive Test Technique Development Based on the Quantitative Prediction of Bond Adhesive Strength," AVSD-0331-70-RR, sponsored by Advanced Research Projects Agency, administered by Naval Air Engineering Center, Warminster, Pa., (July 1970) 110 pgs.

3. Houwink, R. and G. Salomon, Editor, Adhesion and Adhesives, second edition, Vols. I & II, Elsevier Publishing Company, Amsterdam (1965), Chapter 1, Vol. I, pg. 100.

4. Loc. cit. Chapter 1, Vol. I, pg. 95.

5. Schmitz, G. and L. Frank, "Nondestructive Testing for Evaluation of Strength of Bonded Material," prepared for Marshall Space Flight Center under Contract NAS8-11456 by General American Research Division, (September 1965).

6. Schonhorn, H. and L.H. Sharp, Part II, "Chlorotrifluoroethylene Homopolymers and Copolymers," J. Polymer Sci. B2 (1964) 719.

7. Mätting, A. and K. Ulmer, "Grensflachen-Reaktioen and Spannungs - Verteilung in Metall-Klebverbindungen," Elektronen-Austrittsarbeit, Kautschuk Gummi, 16 (1963) 280.

8. Johnson, W.T.M., Part II, "Surface Analysis and Adhesion," Offic. Dig. Federation Soc. Paint Technology, 33 (1961 Nov.).

9. Huntsburger, J.R., "The Locus of Adhesive Failure," J. Poly. Sci. Al, (1963) 1339.

10. Zurbrick, J.R., "Nondestructive Test Technique Development Based on the Quantitative Prediction of Bond Strength," AVSD-0331-70RR, Prepared by Avco Systems Division for the Naval Air Engineering Center, under Contract N00156-69-C-0913 (July 1970).

# APPENDIX I

## SURFACE CLEANING TREATMENTS

SURFACE PREP - ALUMINUM STUDS AND PLATES*

a. Remove oil, grease, etc. by vapor degreasing. Where this is impractical, wipe the faying surfaces clean with cellulose tissues soaked in toluene or methyl ethyl ketone.

b. Immerse for 8 to 12 min in a tap water solution of one of the following alkaline cleaners:

| Cleaner | Concentration | Temperature |
|---|---|---|
| Turco 4215 | 6-8 oz/gal | 150 - 160°F |
| Oakite 61 | 4-8 oz/gal | 160 - 180°F |
| Altrex | 6-8 oz/gal | 160 - 180°F |
| Oakite 164 | 6-8 oz/gal | 160 - 180°F |

c. Rinse thoroughly in water

d. Immerse for 10 to 12 min in a 150 to 160°F solution of the following composition by weight:

| | |
|---|---|
| Demineralized water | 30 parts |
| Sulfuric acid | 10 parts ± 10% |
| Sodium dichromate | 1 part ± 10% |

e. Rinse thoroughly in distilled water either by total immersion so that the final pH will be between 8.5 and 5, or by spray rinse to meet the same pH requirement.

f. Air or oven dry parts at temperatures up to 150°F. Should parts remain unbonded or primed beyond the specified limit (usually 4 to 6 hrs.), they may be returned to the etch tank for a two min "strike", rinsed again, and dried. This will return the surface to a water-break-free condition.

Tank material for this method should be stainless steel lined with polyvinyl chloride, or its equivalent. The tanks should have the equipment necessary to provide a mild agitation to the solution. This is usually accomplished by an air inlet at the bottom of the tank, but filtered or missile-grade air should be used.

In conjunction with a production-type operation, the solutions should be titrated at regular and frequent intervals for proper concentration. A peel specimen is sometimes cleaned, bonded and destructively tested at the beginning of each shift and the results charted. If the chart is closely observed, the indications of an out-of-balance solution will be evident because of the slight decrease in peel values. Water, sodium dichromate, or sulfuric acid may be added when necessary to meet the requirements, but after prolonged use the solution will become dirty or contaminated with foreign matter and must be disposed of and replaced with a fresh mixture.

*Except Special Plates - A2D, A2E, A2F.

Special Plates: After step d, dip quickly in water and wipe dry with clean cloth, then oven dry as with others. The objective is to have an incomplete rinse on these 3 specimens.

NOTES:

1. Notify originator prior to beginning surface prep. Dimension check required.

2. All studs to be sent direct to adhesive lab for priming.

3. All flat specimens to be returned to originator for spectrophotometric measurement before priming.

4. After photometric measurement, all specimens will be returned to adhesives lab for prime and bond.

SURFACE PREP - TITANIUM SPECIMEN PLATES*

A treatment or process which is commercially available that produces excellent bonds with the majority of titanium alloys is as follows:

a. Solvent clean or vapor blast.

b. Immerse 10 to 15 min in the following solution at room temperature:

| | |
|---|---|
| Pasa-Jell 107C | 5 gal. |
| Water | 10 gal. |

NOTE: Solution should be stirred or agitated as required to maintain uniformity.

c. Water rinse thoroughly.

d. Air dry at 65 to 90°F.

e. Prime or bond as soon as possible. If the substrate cannot be primed or bonded within ? hrs, store in polyethylene bags. If over 4 hrs. elapse, recleaning would be in order.

NOTE: Pasa-Jell should be stored in acid-resistant plastic containers or plastic-lined containers. The solution should be discarded after treating 800 sq. in. of titanium per gal of solution.

---

*Except Special Plates: T2D, T2E, T2F

Special Plates - After step b, dip quickly in water and wipe dry with clean cloth. Air dry as with other specimens. The objective is to have an incomplete rinse on these 3 specimens.

NOTES:

1. Notify originator prior to beginning surface prep. Dimension check is required.

2. All specimens to be returned to originator for spectrophotometric measurement before priming.

3. After photometric measurement specimens will be returned to adhesive lab for prime and bond.

SURFACE PREP - STAINLESS STEEL (17-7 PH)*

Method C - The Hydrochloric-Phosphoric-Hydrofluoric Etch

This process is recommended for the 17-7 PH steels, especially where extreme environmental conditions are anticipated.

a. Vapor degrease or solvent clean.

b. Immerse at 170 to 185°F in the following solution:

| | |
|---|---|
| Hydrochloric acid (35%) | 83.3% by volume |
| Phosphoric acid (85%) | 12.5% by volume |
| Hydrofluoric acid (60%) | 4.2% by volume |

c. Spray rinse with demineralized water.

d. Oven dry at 140 to 150°F for 20 to 40 mins.

The tank material should be polyvinyl-chloride-lined mild steel.

---

*Except Special Plates - S2D, S2E, S2F

Special Plates - After step b, rinse quickly and wipe off with clean cloth. Oven dry as with other specimens. The objective is to have an incomplete rinse on these 3 specimens.

NOTES:

1. Notify originator prior to beginning surface prep. Dimension check required.

2. After surface prep, specimens are to be returned to originator for spectrophotometric measurement before priming.

3. After spectrophotometric measurement, specimens will be returned to adhesive lab for prime and bond.